

**Best
Available
Copy**

AD-760 141

UPPER ATMOSPHERIC CHEMICAL RELEASE
TECHNIQUES

H. S. Pergament, et al

AeroChem Research Laboratories, Incorporated

Prepared for:

Rome Air Development Center
Advanced Research Projects Agency

February 1973

DISTRIBUTED BY:

NTIS

National Technical Information Service
U. S. DEPARTMENT OF COMMERCE
5285 Port Royal Road, Springfield Va. 22151

AD 760141

RADC-TR-73-67
Technical Report
February 1973



UPPER ATMOSPHERIC CHEMICAL RELEASE TECHNIQUES

AeroChem Research Laboratories, Inc.

Sponsored by
Defense Advanced Research Projects Agency
ARPA Order No. 1649 Amendment No. 2

Approved for public release;
distribution unlimited.



The views and conclusions contained in this document are those of the authors and should not be interpreted as necessarily representing the official policies, either expressed or implied, of the Defense Advanced Research Projects Agency or the U. S. Government.

Reproduced by
NATIONAL TECHNICAL
INFORMATION SERVICE
U S Department of Commerce
Springfield VA 22151

Rome Air Development Center
Air Force Systems Command
Griffiss Air Force Base, New York

UNCLASSIFIED

Security Classification

DOCUMENT CONTROL DATA - R & D		
(Security classification of title, body of abstract and indexing annotation must be entered when the overall report is classified)		
1. ORIGINATING ACTIVITY (Corporate author) AeroChem Research Laboratories, Inc. P.O. Box 12 Princeton, New Jersey 08540		2a. REPORT SECURITY CLASSIFICATION Unclassified
3. REPORT TITLE Upper Atmospheric Chemical Release Techniques		2b. GROUP
4. DESCRIPTIVE NOTES (Type of report and inclusive dates)		
5. AUTHOR(S) (First name, middle initial, last name) H.S. Pergament, A. Fontijn, W. Felder, D.A. Hatzenbuehler, C.J. Kau		
6. REPORT DATE February 1973	7a. TOTAL NO. OF PAGES ix + 37 46	7b. NO. OF REFS 13
8a. CONTRACT OR GRANT NO. F30602-72-C-0420	9a. ORIGINATOR'S REPORT NUMBER(S) TP-287	
8b. PROJECT NO.	9b. OTHER REPORT NO(S) (Any other numbers that may be assigned this report) RADC-TR-73-67	
10. DISTRIBUTION STATEMENT Approved for public release; distribution unlimited.		
11. SUPPLEMENTARY NOTES Monitored by: J.J. Simons (315)330-3451 Rome Air Development Center (OCSE) Griffiss Air Force Base, NY 13440		12. SPONSORING MILITARY ACTIVITY Advanced Research Projects Agency Washington, DC 20301
<p>The goal of our work under the present contract is to develop preliminary designs of upper atmospheric packages to release Al and Fe (emphasizing Al). The Flashbulb technique, under current investigation, has been previously shown¹ via thermochemical equilibrium calculations to be capable of producing large yields of Al and Fe. An experimental program to determine whether or not these large yields can be practically achieved is in progress. During this report period atomic absorption spectroscopy equipment was set up in the Atlantic Research Corporation vacuum tank for direct measurement of atomic Al and Fe vapor concentrations following Flashbulb releases. Initial small-scale tests to establish feasibility of the technique were unsuccessful. (Measured yields were negligibly small.) However, after consultation with outside experts in solid propellant and pyrotechnic combustion it is believed that changes in mixture formulation to account for the chemical kinetic parameters controlling the combustion process may result in successful Flashbulb releases. These changes include: smaller Al particle diameters (from 50 μ to 2 - 10 μ); smaller Zr particle diameters from 10 - 25 μ to 2 μ); the addition of hydrocarbon binders (e.g. PBAA and</p>		

DD FORM 1473

UNCLASSIFIED

Security Classification

UNCLASSIFIED

Security Classification

14 KEY WORDS	LINK A		LINK B		LINK C	
	ROLE	WT	ROLE	WT	ROLE	WT
Upper Atmospheric Chemical Releases Nucleation/Condensation Pyrotechnic Mixtures						
<p>PBAN) and combustion modifiers (e.g. Fe_2O_3, Cr_2O_3). These new formulations will be tested, within the next few months, via absorption spectroscopy measurements of atomic Al vapor concentrations and collection (of combustion products) techniques in facilities to be set up at AeroChem. In addition to the above measurements, alternate techniques to release Al will be investigated, including; (i) the pyrolysis of some Al-containing alkyl (e.g. TMA) using a packaged liquid propellant-type motor as a heat source, (ii) the use of thermite mixtures (e.g. $\text{Al}_2\text{O}_3 + \text{Zr}$) and (iii) the use of a combustible mixture to vaporize an Al container.</p> <p>The results of preliminary upper atmosphere release package design studies are presented in this report; these include: a parametric series of thermochemical equilibrium calculations, pressure-time history calculations following steady burning and explosive releases and estimates of the position of atomic Fe vapor condensation onset during the expansion of Flashbulb combustion products to ambient pressure. Results of the latter calculations show that homogeneous nucleation will be "frozen" for Flashbulb combustion pressures less than about 10 atm.</p>						

UNCLASSIFIED

Security Classification

UPPER ATMOSPHERIC CHEMICAL RELEASE TECHNIQUES

H. C. Pergament
A. Fontijn
W. Felder
D. A. Hatzenbuehler
C. J. Kau

Contractor: AeroChem Research Laboratories, Inc.
Contract Number: F30602-72-C-0420
Effective Date of Contract: 15 May 1973
Contract Expiration Date: 15 June 1973
Amount of Contract: \$138,450.00
Program Code Number: 3E20

Principal Investigator: Harold S. Pergament
Phone: 609 921-7070

Project Engineer: Joseph J. Simons
Phone: 315 330-3055

Approved for public release;
distribution unlimited.

This research was supported by the
Defense Advanced Research Projects
Agency of the Department of Defense
and was monitored by Joseph J. Simons
RAEC (OCSE), GAFB, NY 13441 under
Contract F30602-72-C-0420.

SUMMARY

The goal of our work under the present contract is to develop preliminary designs of upper atmospheric packages to release Al and Fe (emphasizing Al). The Flashbulb technique, under current investigation, has been previously shown¹ via thermochemical equilibrium calculations to be capable of producing large yields of Al and Fe. An experimental program to determine whether or not these large yields can be practically achieved is in progress. During this report period atomic absorption spectroscopy equipment was set up in the Atlantic Research Corporation vacuum tank for direct measurement of atomic Al and Fe vapor concentrations following Flashbulb releases. Initial small-scale tests to establish feasibility of the technique were unsuccessful. (Measured yields were negligibly small.) However, after consultation with outside experts in solid propellant and pyrotechnic combustion it is believed that changes in mixture formulation to account for the chemical kinetic parameters controlling the combustion process may result in successful Flashbulb releases. These changes include: smaller Al particle diameters (from 50 μ to 2 - 10 μ); smaller Zr particle diameters from 10 - 25 μ to 2 μ); the addition of hydrocarbon binders (e.g. PBAA and PBAN) and combustion modifiers (e.g. Fe_2O_3 , Cr_2O_3). These new formulations will be tested, within the next few months, via absorption spectroscopy measurements of atomic Al vapor concentrations and collection (of combustion products) techniques in facilities to be set up at AeroChem. In addition to the above measurements, alternate techniques to release Al will be investigated, including; (i) the pyrolysis of some Al-containing alkyl (e.g. TMA) using a packaged liquid propellant-type motor as a heat source, (ii) the use of thermite mixtures (e.g. $\text{Al}_2\text{O}_3 + \text{Zr}$) and (iii) the use of a combustible mixture to vaporize an Al container.

The results of preliminary upper atmosphere release package design studies are presented in this report; these include: a parametric series of thermochemical equilibrium calculations, pressure-time history calculations following steady burning and explosive releases and estimates of the position of atomic Fe vapor condensation onset during the expansion of Flashbulb combustion products to ambient pressure. Results of the latter calculations show that homogeneous nucleation will be "frozen" for Flashbulb combustion pressures less than about 10 atm.

FOREWORD

This is the first semi-annual report on Contract F30602-72-C-0420, covering the period 15 May through 31 December 1972. The authors gratefully acknowledge the contributions of A. Macek, S. Scheffee and J. Blevins of Atlantic Research Corporation in helping to formulate the Flashbulb mixtures and obtain the vacuum tank test data.

PUBLICATION REVIEW

This technical report has been reviewed and is approved


RADG Project Engineer

TABLE OF CONTENTS

	<u>Page</u>
SUMMARY	iii
FOREWORD	v
LIST OF FIGURES	viii
I. MEASUREMENTS OF ATOMIC METAL VAPOR YIELDS	1
A. Experimental Setup in ARC Vacuum Tank	1
B. Atomic Absorption Spectroscopy Measurements	1
1. Experimental	1
2. Data Reduction	2
a. Scaling Methods	2
b. Calculation of Number Density from Observed Absorption	3
C. Test Results	7
II. FURTHER TESTING OF FLASHBULB AND ALTERNATE RELEASE TECHNIQUES	8
A. Flashbulb: Al Releases	8
1. Formulation	8
2. Test Facilities at AeroChem	9
a. Small Scale Vacuum Tank	9
b. Larger Scale Atmospheric Pressure Facility	9
B. Alternate Release Techniques	10
III. UPPER ATMOSPHERIC RELEASE DESIGN STUDIES	11
A. Formulation of Flashbulb Mixtures	11
B. Pressure-Time Histories	11
C. Homogeneous Nucleation	12
1. Experimental Data on Fe Condensation	12
2. Rate Coefficient for Dimerization	13
3. Condensation Following Flashbulb Releases	14
D. Heterogeneous Nucleation	15

IV. REFERENCES

Page

17

TABLE I: ARC VACUUM TANK TEST RESULTS

19

LIST OF FIGURESFigure

1	DIAGRAM OF ARC TEST SET-UP	20
2	CALIBRATION (a) AND MEASUREMENT (b) OSCILLOSCOPE TRACES FROM A TYPICAL RELEASE BURN	21
3	GEOMETRY OF BURNING RELEASE	22
4	INFLUENCE OF PATH LENGTH ON NUMBER DENSITY	23
5	INFLUENCE OF MIXTURE RATIO ON PREDICTED ATOMIC Fe VAPOR YIELDS KClO_4 oxidizer	24
6	INFLUENCE OF MIXTURE RATIO ON PREDICTED CHAMBER TEMPERATURE KClO_4 oxidizer	25
7	INFLUENCE OF MIXTURE RATIO ON PREDICTED ATOMIC Fe VAPOR YIELDS NH_4ClO_4 oxidizer	26
8	INFLUENCE OF MIXTURE RATIO ON PREDICTED CHAMBER TEMPERATURE NH_4ClO_4 oxidizer	27
9	INFLUENCE OF MIXTURE RATIO ON PREDICTED ATOMIC Al VAPOR YIELDS KClO_4 oxidizer	28
10	INFLUENCE OF MIXTURE RATIO ON PREDICTED CHAMBER TEMPERATURE KClO_4 oxidizer	29
11	INFLUENCE OF MIXTURE RATIO ON PREDICTED ATOMIC Al VAPOR YIELDS NH_4ClO_4 oxidizer	30
12	INFLUENCE OF MIXTURE RATIO ON PREDICTED CHAMBER TEMPERATURE NH_4ClO_4 oxidier	31

<u>Figure</u>		<u>Page</u>
13	CENTERLINE MACH NUMBER FOR EXPANSION OF SONIC JET INTO VACUUM	32
14	COMPARISONS BETWEEN PRESSURE-TIME HISTORIES FOR STEADY-BURNING AND EXPLOSIVE RELEASES	33
15	RADIUS OF A SPHERE REQUIRED FOR A 20 kg FLASH- BULB EXPLOSIVE RELEASE	34
16	GAS AND PARTICLE TEMPERATURES AND F_e NUMBER DENSITIES IN SHOCK TUBE MEASUREMENTS	35
17	FLOW TIME FOR CONDENSATION ONSET	36
18	POSITION OF CONDENSATION ONSET IN JET	37

I. MEASUREMENTS OF ATOMIC METAL VAPOR YIELDS

A. Experimental Setup in ARC Vacuum Tank

Firings of Flashbulb mixtures of Zr/oxidizer (potassium or ammonium perchlorate)/release metal (Al or Fe) were carried out in the Atlantic Research Corporation high altitude flight facility. The facility comprises an 8 m long cylindrical (1.8 m diam) tank which is evacuated by a five stage steam ejector pumping system. For the firings reported here, at most three stages were operable. This limited the pressures attainable to ≈ 3 Torr with three stages operating; ≈ 14 Torr, two stages; and ≈ 100 Torr, one stage.

Figure 1 shows a schematic of the experimental arrangement. The release package (12)* is horizontally mounted on the axis of the tank at various distances, S, from the transverse analyzing light beam. A 60 cm long cylindrical (15 cm diam) iron pipe shroud (10) holds the release package in a stream of flowing nitrogen purge gas in order to exclude ambient air from mixing with the release products. Ambient oxygen would significantly reduce the observed metal vapor yield by the (fast) reaction, e.g. $\text{Al} + \text{O}_2 \rightarrow \text{AlO} + \text{O}^2$. Alternatively, the entire vacuum tank can be flushed with nitrogen through a 25 cm diam porous plug (15) in the rear wall of the chamber. When this method of purging is used, the rear flange of the shroud is removed.

B. Atomic Absorption Spectroscopy (AAS) Measurements

1. Experimental

The metal vapor yield measurements are made using atomic absorption spectroscopy. The plume of the burning release (13) intersects a collimated light beam from a hollow cathode lamp (1). The metal resonance line and a Ne line (585.2 nm) also emitted by the source are simultaneously monitored using a beam splitter (3) and two monochromators (4) and (5). The light beam is mechanically chopped at 2 kHz (2), and the output signals from the monochromator-mounted photomultiplier tubes (PMTs) are detected using phase-sensitive amplifiers (6) and (7). The net metal atom absorption is obtained as the difference between the attenuation at the metal atom wavelength due to metal atoms plus particulates and the attenuation at the Ne wavelength due to particulates alone. In addition to eliminating the effect of particulate attenuation, this method of differential phase sensitive detection rejects unmodulated background emission levels arising from the highly luminous release vapor of up to 1000 times greater than the lamp intensity.

* Numbers in parentheses in the text refer to Fig. 1.

The metal atom yield measurement by AAS is similar to that used in a portion of the Max Planck Institut (MPI) studies on barium releases.³ However, the MPI studies were made using dc methods, and the net absorption was obtained by subtraction after the experiment. The effect of background emission from the lower temperature Ba thermite releases³ was (unlike the present experiments) apparently negligible and could be ignored. The discrimination and "real-time" data processing capabilities of differential phase-sensitive detection make this method far more suitable for the purposes of the present program than any dc method.

2. Data Reduction

Figure 2 shows tracings of the oscilloscope photographs obtained in release No. 10 (see Table I). The calibration traces (a) for the metal atom (bottom trace) and Ne resonance lines (top trace) give the range of observable absorption. The various sections of the calibration traces are obtained as follows: (1) no absorption in either metal resonance line or Ne line; (2) total absorption of the metal resonance line (monochromator slits closed--note that the Ne line trace is unaffected); (3) total absorption of both the metal resonance line and the Ne line (both monochromator slits closed; note that the metal line attenuation goes to zero--this will be discussed below). After these traces are obtained, the monochromator slits are re-opened and the release is ignited. The experimental traces (b) are begun ≈ 1 sec before ignition and show zero absorption (4) for comparison with the calibration trace. The observed deflection of the metal resonance line in trace (b) is then compared with maximum observable deflection from trace (a) and the fractional transmission I/I_0 is obtained, where I_0 is the maximum deflection obtained from trace (a) and I is the deflection (measured from 100% absorption) obtained from trace (b). The numbers are normalized to an arbitrary scale determined by the maximum deflection of trace (a).

a. Scaling Methods - The fractional transmission can be related to the local number density of metal atoms, N , in the light beam by methods to be described (in b.) below. N is then scaled in the following manner to obtain the total number of atoms released. Assuming that the release plume is approximately a right circular cylinder and that the gas velocity is axial with no transverse components, account is first taken of the fact that only a fraction of the atoms produced pass through the light beam and are observed. This (geometric) scaling factor is the ratio of the volume of the light beam in the release plume to the volume of the cylinder swept out by rotating the light beam about the axis of the release plume,

$$\frac{\text{Atoms detected}}{\text{Atoms produced}} = \frac{\frac{\pi w^2 l}{4}}{\frac{\pi l^2 w}{4}} = \frac{w}{l}$$

where w is the diameter of the light beam (2.5 cm for these experiments) and l is the optical path through the release plume (see Fig. 3). Second, account is taken of the fact that the measured absorption corresponds to the density in the absorbing path for only a time period equal to the gas flow time (i. e. time for an atom to traverse the light beam). Since the release formula- tion burns for a much longer time a (temporal) scaling factor is formulated which is the ratio of the flow time to the burning time.

$$\frac{\text{Flow time}}{\text{Burning time}} = \frac{\pi w/4 \cdot v_g}{t_b}$$

where v_g is the gas velocity in the plume and t_b is the release burning time. Finally, we convert the number density (ml^{-1}) to the total number of atoms produced by multiplying by the observation volume, $\pi w^2 l/4$. These scaling factors result in the following expression for n_{tot} , the total number of atoms released as vapor,

$$n_{\text{tot}} \approx N \cdot \left(\frac{l}{w}\right) \cdot \left(\frac{4v_g}{\pi w}\right) t_b \cdot \frac{\pi w^2 l}{4} = N \cdot l^2 v_g t_b$$

In this expression, l is obtained from a visual estimate of the luminous plume diameter at the optic axis; v_g is calculated from a gas dynamic analysis of the release plume; and t_b is taken directly from the experimental oscillo- scope trace (cf. Fig. 2, Trace b).

b. Calculation of Number Density from Observed Absorption - In this section we present the relationships between the measured light absorp- tion and the number density, N . Two cases, low ($< 10^{15} \text{ ml}^{-1}$) and high ($> 10^{15} \text{ ml}^{-1}$) atom densities will be distinguished. In these regimes the absorp- tion processes differ, and consequently the experimental methods and analy- ses are different. For the purposes of our experiments, the measurement of low atom densities is in the nature of a feasibility demonstration. A success- ful release should yield metal atom densities in excess of the limit of validity of the low density (resonance line absorption) measurement technique. We present below the analysis to derive N from a resonance line absorption mea- surement, discuss the limitations of this technique, and describe the method

we will use for measuring large metal atom densities.

- (1) Low Densities - For a resonance line source the Beer-Lambert law gives the relationship between fractional light transmission, I/I_0 , through an absorbing path of length ℓ , and the density of absorbers, N :

$$I/I_0 = \exp(-k N \ell) \quad (1)$$

or

$$N = \ln(I_0/I) \cdot \left(\frac{1}{k\ell} \right)$$

where k is the resonance line absorption coefficient at the line center given by the well-known⁴ formula

$$k = \left(\frac{\pi M}{RT} \right)^{1/2} \cdot \frac{e^2 f}{m_e \nu_0}$$

where ν_0 is the absorption line frequency, f , the absorption oscillator strength, e and m_e , the electronic charge and mass, respectively, M , the atomic mass of the absorber, R , the universal gas constant, and T , the absolute temperature. Substituting the values for the 371.9 nm Fe line and the 396.2 nm Al line,⁵ we obtain

$$N_{\text{Fe}} = \frac{(4.6 \times 10^{11})}{\ell} \ln(I_0/I)$$

$$N_{\text{Al}} = \frac{(3.7 \times 10^{11})}{\ell} \ln(I_0/I)$$

Only these first order relationships are used to determine N because of the limited purpose of the resonance line measurements and because of the limitations on the validity of the method, discussed below.

Basically, resonance line absorption is an invalid technique for determining atom densities when the absorption linewidth becomes dependent on atom concentration. This occurs at high absorber densities where interactions between the absorbing atoms broaden the absorption line (i.e., Holtzmark broadening) and overwhelm density-independent mechanisms (Doppler and natural broadening). For Al, the densities at which Holtzmark broadening begin to dominate the linewidth⁶ are $\approx 10^{15} \text{ ml}^{-1}$ for the strong 396.2 nm line and $\approx 10^{16} \text{ ml}^{-1}$ for the 219.9 nm line which corresponds to one of the weakest

transitions from the ground state. We note that, although the ratio⁴ of the f-numbers of these transitions is $\approx 10^2$, only a factor of 10 in range is gained by using the weaker line because the onset of Holtzmark broadening is, to a first approximation, proportional^{6,7} to $f^{1/2}$.

Furthermore, above 90% absorption, large concentration changes yield only small changes in the percentage absorption, and the measurement of these small changes becomes increasingly inaccurate (e.g. the 5% increase in absorption between 90 and 95% corresponds to a 30% increase in atom density). Taking 90% absorption as an experimental upper limit, the maximum Al atom densities which can be reliably measured across a 1 cm path by line absorption are $\approx 10^{12} \text{ ml}^{-1}$ at 396.2 nm and $\approx 10^{15} \text{ ml}^{-1}$ at 219.9 nm.

- (2) High Densities - To measure atom densities in excess of 10^{15} ml^{-1} we take advantage of the Holtzmark broadening of the absorption line. A continuum source is used, and a variable bandpass monochromator is set at the metal atom resonance line. The bandpass of the monochromator is adjusted to the maximum expected metal linewidth (e.g. $\approx 0.5 \text{ nm}$ half width at $[\text{Al}] = 10^{17}$ and $\lambda = 396.2 \text{ nm}$) and the absorption is measured in the same manner as the resonance line source. (As before, the second monochromator views the light source at a non-resonance wavelength, and the net metal atom absorption is obtained using differential amplification.) Setting the monochromator resolution equal to or just larger than the anticipated linewidth allows the entire absorption band to be detected (i.e., with a continuum source, absorption is measured throughout the entire bandwidth as opposed to a line source where absorption is measured only at the band center). Since the total transition moment remains constant (independent of linewidth), the absorption again follows the Beer-Lambert law, Eq. (1).

For analyzing these measurements, we use the absorption coefficient, k_H , for Holtzmark broadening given by Brunner:⁶

$$k_H = \left(\frac{\pi e^2}{m_e c^3} \right) f(\gamma_N + AfN) \lambda_0^4 / (\Delta \lambda)^2 \quad (2)$$

where c is the velocity of light; λ_0 , the resonance line center wavelength; $\Delta \lambda = \lambda_0 - \lambda$; γ_N the natural damping constant;

and $A = 1.92 e^2 \lambda_0 / m_e c (g_u / g_l)^{1/2}$, where g_u and g_l are the statistical weights of the upper and lower states, respectively. The Beer-Lambert law is now written as

$$I/I_0 = \int_0^\infty \exp(-k_H N \ell) d\lambda \quad (3)$$

where the integration over wavelength is performed to account for the finite width of the absorption line. In addition, since the transmission of the monochromator is not constant across the absorption linewidth, a slit function must be used to weight the expression for net absorption. We have approximated the triangular slit function, S , of our monochromator by a gaussian

$$S(R, \Delta\lambda) = \frac{2.345}{(2\pi)^{1/2} R} \exp\left[-\frac{1}{2} \left(\frac{2.345 \Delta\lambda}{R}\right)^2\right] \quad (4)$$

where R is the nominal resolution of the monochromator (reciprocal dispersion \times slit width), 0.5 nm halfwidth. Equation (2) now becomes

$$I/I_0 = \int_{-\infty}^{\infty} \exp(-k_H N \ell) \cdot S(R, \Delta\lambda) d\Delta\lambda \quad (3a)$$

Figure 4 shows the results of calculations of this integral for path lengths, ℓ , of 1, 10, and 25 cm. This figure will be used to obtain N from measured values of I/I_0 and the estimated path length,

Finally, we note that for both the resonance and Holtzmark absorption calculations it has been implicitly assumed that the absorber density is uniform across the light path, ℓ . For resonance line absorption, this assumption is immaterial because the nature of the absorption process is density-independent. On the other hand, the onset of Holtzmark broadening and the broadened linewidth are both density-dependent. Explicit forms for $N(\ell)$, obtained from a gas dynamic analysis of the release plume, should therefore be used in Eqs. (2) and (3a).

C. Test Results

Twenty-six firings were made in the ARC vacuum tank in an effort to demonstrate initial feasibility (15 contained Al and the remainder, Fe) of the Flashbulb technique. Twenty-four firings were made as strand-type burns at ambient (tank) pressure; the other two were made using nozzles to fix the combustion pressure at 1 atm. Initially, firings were made using KClO_4 oxidizer (5 firings). NH_4ClO_4 was later found to have more controllable burning characteristics and it was used for the remaining tests. In addition, for the reasons cited previously, after the first 5 firings the N_2 shroud was incorporated.

Table I contains a summary of all the tests. Atomic metal vapor yield data were obtained in only 11 firings because of the various experimental problems listed in the table.* As noted in Table I, the measured yields are negligibly small--on the order of 10^{-5} to 10^{-4} %--and no meaningful trends (e.g. variation in yield with combustion pressure, mixture mass, etc.), can be observed. However, it should be pointed out that these initial tests were performed in a rather non-systematic manner in the hope of demonstrating small-scale feasibility of the Flashbulb technique directly without undertaking a solid propellant (or pyrotechnic) type development program. The results in Table I clearly show the pitfalls of this approach.

* These problems included failure to ignite, poor synchronization of the measurement trace with the burn period because of ignition delay, overloading of the discrimination capability of the tuned amplifier due to high plume luminosity, 100 % attenuation of the light beam due to particulates and saturation of the detection electronics due to high light levels. All of these problems are amenable to direct solutions and pose no insurmountable difficulties. The most serious interferences with the measurements are the high plume luminosity and/or 100 % attenuation due to particulates; both of these problems can be solved by increasing the distance from the release to the optic axis and/or decreasing the effective optical path by means of baffles.

II. FURTHER TESTING OF FLASHBULB AND ALTERNATE RELEASE TECHNIQUES

A. Flashbulb: Al* Releases

After an in-house review of the test data and consultation with outside experts[†] in solid propellant and pyrotechnic combustion it has become clear that more consideration should have been given to basic chemical kinetic parameters and internal ballistics of the burning release, and that such factors as metal particle size, particle residence time in the hot gas zone, amount of gas produced, heat losses, etc., were the limiting parameters in these tests. We therefore plan to continue testing the Flashbulb concept, in test facilities at AeroChem, with significant modifications in mixture formulation, including the use of (i) smaller Al particle diameters ($2\text{-}10\mu$) than were used during the ARC tests, (ii) smaller Zr particle diameter (2μ) than previously used, (iii) hydrocarbon binders, and (iv) combustion modifiers.

1. Formulation

A series of Flashbulb mixtures (ranging in size from 10 to about 100 g) will be formulated for testing at AeroChem. The parameters to be varied in the formulation are:

Zr particle size: 2μ
 Al particle size: from 2μ to 10μ
 Wt. % Al: ≈ 5 to 25 %
 Binders: (≈ 5 to 10 wt. %) e.g.
 PBAA-polybutadiene acrylic acid
 PBAN-polybutadiene acrylic nitrite
 Combustion modifiers: (≈ 1 wt. %) e.g. MnO_2 , Fe_2O_3 , Cr_2O_3 ,
 SnO_2

These mixtures will be compounded at Picatinny Arsenal, Dover, N.J.

* Only Al will be released for the remainder of this program, since it appears to be more important than Fe for practical applications.

† Prof. I. Glassman (Princeton University), E. Price (Naval Weapons Center), Prof. D.E. Rosner (Yale University) and several personnel at Picatinny Arsenal.

Because of the small release packages to be tested, heat losses will be larger and residence times smaller than in full scale releases; thus we do not expect the test results to approach the thermodynamically predicted yields. Atomic metal vapor yields of about 1% from the small scale packages would be considered acceptable to demonstrate feasibility of the technique for use in full scale (say 20 kg) upper atmospheric releases. If acceptable yields are obtained, a scale model test program will be required to develop full scale upper atmospheric release packages. If, however, yields of about 1% cannot be achieved by a suitable combination of the formulation parameters, the Flash-bulb technique will be declared dead, and our efforts will switch to the most promising alternate release technique (see below).

2. Test Facilities at AeroChem

- a. Small Scale Vacuum Tank - An existing vacuum system will be modified for testing release packages of up to 10 g. It will consist of a 2.5' long, 10" diam stainless steel lower section (to hold the release package) and an upper glass section 3' long, 1.5' diam lined with Mo or stainless steel sheet. Optical measurements will be made through ports located at the midpoint of the glass portion; provision will also be made for collection of the release products. The vacuum facility is pumped by a 300 cfm mechanical pump and can attain ultimate pressures of ≈ 10 mTorr. Provision will be made for purging the facility with various inert gases at known flow rates.
- b. Larger Scale Atmospheric Pressure Facility - We plan to test samples of up to 100 g. However, safety considerations and pumping restrictions preclude testing these samples in the small vacuum facility. We will therefore construct a simple, atmospheric pressure flow tube flushed with Ar or N₂ to make yield measurements on the larger samples via AAS. No essential information about the atomic metal vapor yield is lost by working at an ambient pressure of 1 atm. The combustion pressure and particle residence times will be controlled by the orifice diameter and canister configuration. No information about metal vapor condensation during expansion of the exhaust gases into vacuum will, of course, be obtained from these tests. The flow tube will be housed in an existing propellant test shed at AeroChem and will be vented to the atmosphere.

B. Alternate Release Techniques

Some alternate techniques considered for the release of atomic Al in the upper atmosphere include: the use of thermite mixtures (e.g. $\text{Al}_2\text{O}_3 + \text{Zr}$), use of a combustible mixture to vaporize an Al container, and the pyrolysis of some Al-containing alkyl (e.g. TMA) using a packaged liquid propellant-type motor as a heat source.

At this point the last scheme appears to be most promising on the basis of thermochemical equilibrium calculations which show that at temperatures above about 2000 K almost all the Al in TMA is atomic Al vapor. However, there are many additional factors which must be taken into account, e.g.,

1. The liquid propellant combustion products should be non-oxidizing.
2. Can a practical method be found to inject TMA into the combustion chamber?
3. Can the equilibrium concentration of atomic Al vapor be achieved practically when TMA is injected into the chamber?
4. What is the total payload required to release significantly large amounts of Al?
5. Can we use existing packaged liquid propellant systems, or should we consider e.g. cyanogen/oxygen flames, which produce very high temperatures (≈ 4000 K) with very high ratios of $[\text{Al}]/[\text{AlO}]$?

We plan to start investigating the practicality of this scheme immediately.

III. UPPER ATMOSPHERIC RELEASE DESIGN STUDIES

Two of the major problems in obtaining a large atomic metal vapor cloud following an upper atmospheric release are, (i) to achieve large atomic metal vapor concentrations at the pressure at which the vapors are produced (for Flashbulb this is the combustion pressure) and (ii) to prevent condensation during the expansion of the metal vapors to ambient pressure. These problems are, of course, common to all releases and much of our work, particularly nucleation/condensation effects, will be generally applicable and not restricted to Flashbulb.

A. Formulation of Flashbulb Mixtures

Additional thermochemical equilibrium calculations have been made to determine optimum combustion pressures and mixture ratios for maximum atomic Al and Fe vapor yields. Figures 5 through 12 show atomic metal vapor yields and combustion temperatures as a function of chamber pressure for both KClO_4 and NH_4ClO_4 oxidizers. The oxidizer was switched from KClO_4 to NH_4ClO_4 (see Section II) for several reasons: (i) the burning rate exponent* was found (experimentally) to be reduced from unity to about 0.6, which therefore makes it possible to operate the mixture as a solid propellant (see e.g. Ref. 8), i.e. in a closed canister -- with an orifice (ii) much practical experience has been obtained with NH_4ClO_4 as an oxidizer in propellants, and (iii) ion concentrations are reduced when using NH_4ClO_4 , thus reducing the rate of heterogeneous nucleation (see Section D below).

Figures 5, 7, 9, and 11 show that the theoretical yield is a strong function of both mixture ratio and combustion pressure, but is only slightly affected by changing the oxidizer. A cross plot of the results at constant pressure would show a peak in Al (and Fe) vapor yield; the value of n at which the peak occurs depends on the pressure. On the other hand, at constant n , the yield increases asymptotically to a maximum value as pressure decreases. Combustion temperatures decrease with decreasing pressure and with increasing values of n (because the release metal acts as an inert in this mixture). These results can be used to perform design trade-off studies in which mixture ratio and combustion pressure are the parameters.

B. Pressure-Time Histories

The pressure-time (or distance, in the Lagrangian sense) history of the metal vapors as they expand from the Flashbulb combustion pressure to

* Burning rate exponent \bar{n} is defined from, $\dot{r} \propto p^{\bar{n}}$ where \dot{r} is the burning velocity and p is pressure.

ambient pressure is important input data to the determination of nucleation/condensation rates. Larger values of the pressure/time derivative and lower absolute values of pressure generally favor lower nucleation rates and possible "freezing" of the homogeneous and heterogeneous nucleation processes. In this section we show the results of pressure-time history calculations for two potential release modes, i.e. steady burning and explosive releases. In the steady burning release we envision the Flashbulb mixture burning in a canister with a sonic orifice--venting to ambient for the total combustion time (on the order of, say, 10 sec). Centerline pressures are computed (assuming isentropic flow) from the Mach number distribution along the centerline of a jet expanding into vacuum, as determined by Ashkenas and Sherman⁹ (see Fig. 13). In the explosive release the Flashbulb mixture is assumed to be burned within a closed container (a "bomb") which would burst at a predetermined combustion pressure. Typical combustion times would be on the order of, say, 1×10^{-3} sec. The vapor/particle cloud is then assumed to expand spherically to ambient pressure with the limiting velocity,* $(2/\gamma - 1)a$, where a is the local speed of sound.

Pressure-time histories are compared in Fig. 14 for both release modes for initial (combustion) pressures of 1, 10 and 100 atm. The initial pressure drop for the steady burning release is attributable to the fact that the pressure at the orifice is less than the combustion pressure by about a factor of 2. However within a short time period the curves cross and the explosive release is observed to expand more rapidly than the steady burning release.

It is probable that explosive releases would generally have larger combustion pressures than steady burning releases (for a fixed release mass) because of size limitations. For example, Fig. 15 shows that to release a 20 kg Flashbulb mixture at a pressure of 100 atm requires a sphere 4 ft in diameter to contain the combustion gases. A steady burning release, on the other hand, could easily be operated at the same combustion pressure with a canister of much smaller volume.

C. Homogeneous Nucleation

1. Experimental Data on Fe Condensation

The only available experimental data on condensation of Fe vapor in expanding flows[†] are those of Kung and Bauer.¹⁰ In their shock tube studies

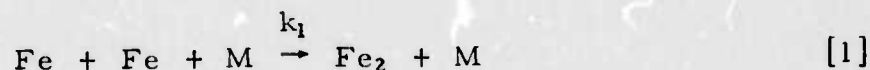
* This is actually the velocity of the contact surface, which follows the shock wave (formed by the explosion) into vacuum.

† No data are available on condensation of Al vapor in expanding flows.

iron vapor was generated by thermal decomposition of 0.5 mole % $\text{Fe}(\text{CO})_5$ in Kr at an initial pressure of 50 Torr. Unsaturated Fe vapor was obtained immediately downstream of the reflected shock at a temperature of approximately 2600 K. Typical data are shown in Fig. 16. The variation of monomer number density deduced from the pressure trace (i.e. the monomer number density for no condensation) is shown in curve 1. The cluster temperature and gas temperature, deduced from emission traces, are given by curves 2 and 3, respectively. Curve 4 (emission trace) gives the number of Fe atoms in the condensed phase, and curve 5, the difference between curves 1 and 4 shows the variation of the actual monomer concentration. The point of "condensation onset" (which occurs approximately 10^{-3} sec after arrival of the expansion fan (point E)), as defined by the intersection of the dashed lines extending from curve 4, is noted to fall very close to the point of 10% monomer consumption.

The Kung and Bauer measurements¹⁰ provide important data for two preliminary studies:

1. Estimation of the rate coefficient for the three-body dimerization reaction of Fe vapor



2. Development of a computational model for prediction of condensation onset following Flashbulb releases in the upper atmosphere.

2. Rate Coefficient for Dimerization

Formation of the dimer is the slowest step for homogeneous nucleation since it occurs only through termolecular collisions. Once the dimer is formed, larger clusters can be produced by bimolecular collisions. Therefore, if we assume that the rate determining step for producing the clusters observed by Kung and Bauer¹⁰ is $\text{Fe} + \text{Fe} + \text{M} \rightarrow \text{Fe}_2 + \text{M}$ then the measured condensation onset time can be used to infer a maximum value for the dimerization rate coefficient,* k_1 .

If the variation of pressure and temperature is neglected, k_1 may be evaluated from†

$$k_1 = \frac{1}{[\text{Fe}]} - \frac{1}{[\text{Fe}]_0} [\text{M}] (t - t_0) \quad (5)$$

* A similar analysis has been performed by Golomb et al¹¹ for condensation of N_2 , Ar and other gases in free jets.

† Note that this interpretation assumes the back reaction proceeds at a negligible rate and therefore results in an upper limit of k_1 .

where subscript "o" stands for initial conditions, i.e. point E in Fig. 16, $[M]$ is number density, and t is time. The rate coefficient corresponding to a 10% consumption of Fe monomer in 10^{-3} seconds has been computed from Eq. (5) to be,*

$$k_1 = 8.3 \times 10^{-34} \text{ ml}^2 \text{ molec}^{-2} \text{ sec}^{-1}$$

at a temperature of 2500 K. The dependence of k_1 on temperature cannot be obtained from the above experimental data. However, it is reasonable to assume

$$k_1(T) \propto T^{-n} \quad (6)$$

where n varies, typically, from 1 to 2, since from classical reaction rate theory the termolecular association reactions have been found to have a negative temperature dependence.

3. Condensation Following Flashbulb Releases

Condensation of Fe (or Al) vapor along a streamline (following a steady burning Flashbulb release from a canister) can be determined from

$$\frac{dX}{dS} = \frac{DW}{\rho u} \dot{w} \quad (7)$$

where X is the local mole fraction of Fe monomer, S is downstream distance nondimensionalized by the orifice diameter, D , and W , ρ and u are molecular weight (assumed to be constant), density and velocity of the gas mixture, respectively. No contributions from flow diffusion processes are considered here. The monomer depletion from the dimerization process is given by

$$\dot{w} = -k_1(T) \frac{\rho^3}{W} X^2 \quad (8)$$

Integrating Eq. (7) along a streamline and using the standard isentropic relations between temperature, pressure and Mach number gives,

$$\frac{1}{f} = 1 + \frac{DX_0}{a_0} \left(\frac{P_0}{RT_0} \right)^2 \int_0^S k_1(T) \left(1 - \frac{\gamma-1}{2} M^2 \right)^{\frac{-(5-\gamma)}{2(\gamma-1)}} M^{-1} dS \quad (9)$$

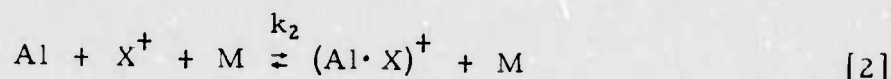
* It is reasonable to assume that this rate coefficient can also be used for the reaction, $\text{Al} + \text{Al} + \text{M} \rightarrow \text{Al}_2 + \text{M}$, in subsequent estimates of the location of condensation onset for Al.

where $f = X/X_0$, γ is the ratio of specific heats, M is the Mach number, R is the universal gas constant, and P_0 , T_0 , a_0 and X_0 are pressure, temperature, speed of sound and Fe mole fraction in the chamber. The results obtained for the location of condensation onset from Eq. (9) will be conservative (i.e. condensation onset will be predicted at smaller values of S than expected in an actual release) since (i) the reverse of Reaction [1] is neglected and (ii) no account is taken of whether, in fact, the initial flow is supersaturated. Thus, if by using the 10% monomer decay ($f = 0.9$) as a criterion, condensation onset is not predicted from Eq. (9), it is doubtful that condensation will be a problem. Using the Mach number distribution shown in Fig. 13, Eq. (9) was integrated numerically for a typical set of Flashbulb release conditions. The predicted points of condensation onset (i.e. $f = 0.9$) are plotted on (P_0, t) and (P_0, S) planes in Figs. 17 and 18, respectively, assuming $k_1 \propto T^{-2}$. The chamber temperatures, T_0 , for these cases ranged from 3910 K to 4170 K and initial Fe mole fractions were approximately 0.55 for chamber pressures from 15 atm to 50 atm; the orifice diameter was taken to be 1 ft.

Since the termolecular collisions depend strongly on concentrations of the participating monomer, the strong dependence of condensation onset on chamber pressure is expected. For these releases no condensation (based on homogeneous nucleation) is predicted for chamber pressures less than about 20 atm.

D. Heterogeneous Nucleation

Data on the heterogeneous nucleation of atomic Al and Fe via ions are apparently unavailable. To estimate the effect of this process, we have analyzed the available data for the rate limiting step in similar processes, i.e. the termolecular formation of a cluster



The forward rate of this reaction will depend upon the nature of X^+ and the polarizability, α_{Al} , of Al. The larger the radius of the ion, the smaller will be the attractive force between it and Al, resulting in a smaller rate; the larger the polarizability of the neutral Al, the larger will be the attractive force, resulting in a larger rate. A contour map relating rate constants and equilibrium constants to polarizability and ionic mass for alkali ion clustering has been constructed by Keller and Niles.¹² Making the reasonable assumption that $\alpha_{\text{Al}} \leq \alpha_{\text{alkali}} \approx 10^{-23} \text{ cm}^3$,¹³ and using the mass range 20-80 amu for the ion, the contour map gives a forward rate constant $k_2 \approx 5 \times 10^{-29} \text{ ml}^2 \text{ molec}^{-1} \text{ sec}^{-1}$ as an upper limit at 300 K. At 2500 K, $k_2 \approx 1.5 \times 10^{-30} \text{ ml}^2 \text{ molec}^{-1} \text{ sec}^{-1}$ (assuming a $T^{-3/2}$ dependence). Comparing this rate coefficient with that

obtained for homogeneous nucleation above (both rate coefficients represent reasonable upper limits, irrespective of species) we find that, $k_2/k_1 \approx 10^{-30}/10^{-33} = 10^3$. Thus, to a first approximation, ionic nucleation will compete with homogeneous nucleation as a loss process only if $X_{\pm}/X_{Al} > 10^{-3}$, where X_{\pm} and X_{Al} are gas phase mole fractions of charged species* and Al in the release products, respectively. Our present estimates of ion densities, from thermodynamic equilibrium calculations in Zr/NH₄ClO₄/Al systems, indicate that $X_{\pm}/X_{Al} \approx 10^{-4}$, so that ionic nucleation appears to be a factor of 10 less prominent as a monomer removal process than homogeneous nucleation.

A third nucleation mechanism, heterogeneous nucleation on particles, will also play a role in atom losses. Data for this process are, as in the case of ionic nucleation, not available. However this loss process can be analyzed in terms of elementary kinetic theory by calculating the encounter rate between metal atoms and solid (or liquid) particles in the release plume. Monomer loss rates can then be estimated assuming various fractional "sticking" efficiencies. In order to perform these estimates, reasonable assumptions about the average particle sizes, velocities, and temperatures must also be made. The estimated particle nucleation rates can then be compared with the gas-phase rates calculated above to determine the dominant monomer loss process(es) and to suggest changes (if necessary) in the Flashbulb mixture formulations and/or release conditions.

* As a first (and most conservative) estimate, we include all charged species, both positive and negative, and assign the same (large) rate constant.

IV. REFERENCES

1. [REDACTED]
2. Fontijn, A. and Kurzius, S.C., "Tubular Fast-Flow Reactor Studies at High Temperatures. I. Kinetics of the Fe/O₂ Reaction at 1600 K," Chem. Phys. Letters 13, 507-510 (1972); see also Fontijn, A., Felder, W. and Houghton, J.J., "Kinetics of Metal Atom Oxidation Reactions," AeroChem TN-151, Semi-Annual Technical Summary Report, November 1972.
3. Brunner, W., Foppl, H. and Michel, K.W., "Vaporization of Metals in Two-Phase Jets with Various Modes of Energy Deposition," Astronaut. Acta 15, 613-624 (1970).
- i. Mitchell, A.C.G. and Zemansky, M.W., Resonance Radiation and Excited Atoms (Cambridge Univ. Press, New York, 1961; reprint of 1934 edition) chap. III, pp. 47-103.
5. Wiese, W.L., Smith, M.W. and Miles, B.M., Atomic Transition Probabilities, NSRDS-NBS 22 (National Bureau of Standards, Washington, October 1969).
6. Brunner, W., "Absorptionsspektroskopie an resonanzverbreiterten Atomlinien zur Dichtemessung in Dusenstrahlen," Z. Naturforsch. 24A, 1063-1065 (1969).
7. Ali, A.W. and Griem, H.R., "Theory of Resonance Broadening of Spectral Lines by Atom-Atom Impacts," Phys. Rev. 140A, 1044-1049 (1965); Errata, Phys. Rev. 144A, 366(1966); Lortet, M.C. and Roueff, E. "Broadening of Hydrogen Lines in a Neutral Medium," Astron. Astrophys. 3, 462-467 (1969).
8. Hugget, C., "Combustion of Solid Propellants," High Speed Aerodynamics and Jet Propulsion, Vol. II, Combustion Processes (Princeton Univ. Press, Princeton, 1956).
9. Ashkenas, H. and Sherman, F.S., "The Structure and Utilization of Supersonic Free Jets in Low Density Wind Tunnels," Rarefied Gas Dynamics, Vol. II, ed. J.H. de Leeuw (Academic Press, New York, 1966) pp. 84-105.

10. Kung, R.T.V. and Bauer, S.H., "Nucleation Rates in Fe Vapor: Condensation to Liquid in Shock Tube Flow," presented at Eighth International Shock Tube Symposium, Imperial College of Science and Technology, London, 5-8 July 1971.
11. Golomb, D., Good, R.E., Bailey, A.B., Busby, M.R., and Danbarn, R., "Dimers, Clusters and Condensation in Free Jets. II.," J. Chem. Phys. 57, 3844-3852 (1972).
12. Keller, G.E. and Niles, F.E., "Labile Clustering and Its Effects," Chem. Phys. Letters 10, 526-529 (1971).
13. Bederson, B. and Robinson, E.J., "Beam Measurements of Atomic Polarizabilities," Advances in Chemical Physics, Vol. X, Molecular Beams, ed. J. Ross (Wiley Interscience, New York, 1966).

TABLE I. ARC VACUUM TANK TEST RESULTS

Compositions: wt. %												
			Zr	KClO ₃	NH ₄ ClO ₃	Fe	Al					
	X	48	31	---	---	21	---					
	Y	40.4	---	23.4	36.2	---	---					
	Z	47.1	---	27.5	---	25.4	---					

Run No.	Composition	Release Mass (g)	Metal Particle Size (μ)	Zr Particle Size (μ)	Burn Time (sec)	Ambient (Tank) Pressure (Torr)	N ₂ Flow (g/sec)	Distance to Optic Axis (in.)	% Absorption (max)	Total No. Atoms Released	% Yield ^b	Comments
1	X	10	50	10	---	100	0	3.5	---	---	---	Vertical mounting; test run - overload
2	X	10	50	10	35	13	0	38	< 15	---	---	No permanent record; film overexposed
3	X	10	50	10	?	100	0	38	15 - 25	?	?	Uncertain burn time; no yield calculation
4	X	10	50	10	?	100	0	32	15	?	?	Uncertain burn time; no yield calculation; overload
5	X	10	50	10	2	100	0	44	18 - 24	10 ¹⁷	5x10 ⁻⁴	Momentary overload, very bright flash at ≈ 2 sec
6	Y	10	50	10	3	14	0	36	---	---	---	Missed synchronization - no record
7	Y	10	50	10	1	14	0	30	---	---	---	"
8	Y	10	50	10	2	13	3.0	24	12	3 x 10 ¹⁶	3x10 ⁻⁵	Shroud purge
9	Y	10	50	10	2	14	3 (off)	3.5	80	5 x 10 ¹⁷	5x10 ⁻⁴	Flow N ₂ through shroud for 30 sec, turn off and fire.
10	Y	10	50	10	2	14	3 (off)	3.5	80	5 x 10 ¹⁷	5x10 ⁻⁴	"
11	Z	10	50	10	5	13	3	16	---	---	---	Shroud purge
12	Z	10	50	10	5	14	10	6	12	10 ¹⁷	6x10 ⁻⁵	Shroud purge
13	Z	10	50	10	5	14	3	3	90	6 x 10 ¹⁷	3x10 ⁻⁴	Shroud purge
14	Z	10	50	10	2	13	1	3	50	4 x 10 ¹⁷	2x10 ⁻⁴	Shroud purge, ignite both ends of strand - saturation
15	Z	10	50	10	4	13	1.5	5	---	---	---	Shroud purge - attenuation < 10%
16	Z	10	50	10	4	14	1.5	3.5	---	---	---	"
17	Z	33.3	30	< 25	1	4	30	3.5	30	3 x 10 ¹⁶	10 ⁻⁶	Tank purge; -400 mesh Zr = particles < 25μ diam.
18	Z	100	30	< 25	2	3	30	4	25	4 x 10 ¹⁶	2x10 ⁻⁴	1 atm combustion pressure from nozzle
19	Z	100	30	< 25	2	3	30	16	50	10 ¹⁷	5x10 ⁻⁶	Tank purge; collector foil at 12' on axis showed particle impacts
20	Z	100	50	10	6.5	760	3	4	---	---	---	Shroud purge; particulate attenuation near 100%.
21	Z	100	50	10	6.5	760	3	16	---	---	---	overload after particulates cleared; large deposit of fine white powder all over tank.
22	Z	100	50	10	5.5	760	3	36	---	---	---	100% particulate attenuation; shroud purge
23	Z	100	50	10	13	160	3	36	---	---	---	Faulty setup: λ metal set wrong - no data
24	Z	33.3	30	< 25	1	125	3	30	---	---	---	Very bright - overload; shroud purge
25	Z	100	10	< 25	2	125	3	30	---	---	---	Very bright - overload; shroud purge
26	Z	100	10	< 25	1.5	760	3	36	30	2 x 10 ¹⁶	10 ⁻⁶	Very bright; partial overload at ≈ 1 sec

a All strand-type burns with combustion pressure equal to ambient (tank) pressure except Run Nos. 18 and 19 which had nozzles to fix the combustion pressure at 1 atm.

b % Yield = $\frac{\text{Mass of metal released as vapor}}{\text{Total mass of release (col. 5)}} \times 100$

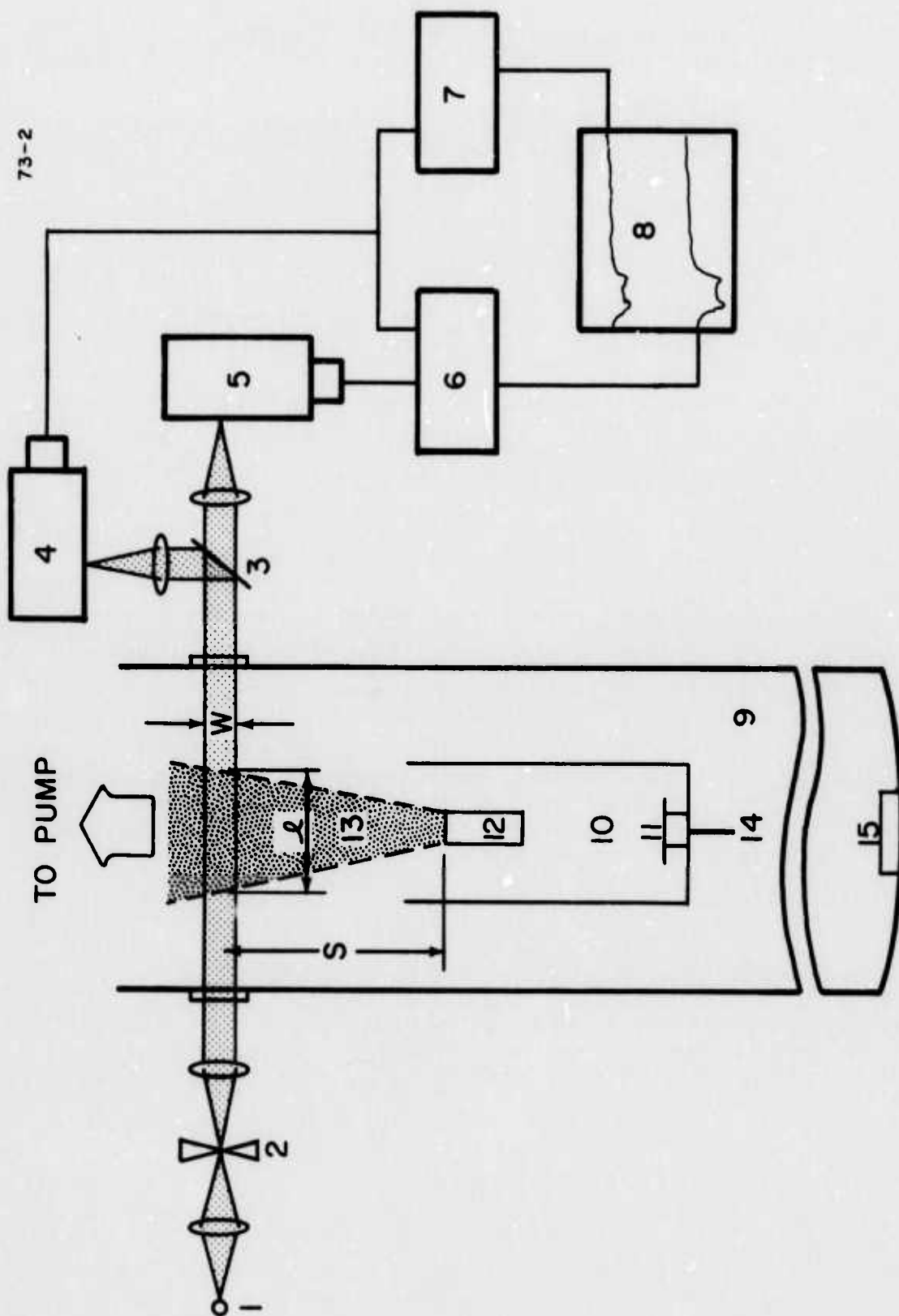


FIG. 1 DIAGRAM OF ARC TEST SET-UP

FIG. 1 DIAGRAM OF ARC TEST SET-UP

Key

Optics (1-3): 1, light source; 2, kHz chopper; 3, beam splitter.

Differential Phase-Sensitive Detection

System (4-8): 4, monochromator and PMT set at Ne line (585.2 nm);
5, monochromator-PMT set at metal atom resonance line
(372. nm, Fe; 396.2 nm, Al); 6, differential tuned
amplifier to give net metal atom absorption (see text);
7, tuned amplifier to give particle absorption and scattering
(see text); 8, dual beam oscilloscope; upper trace, particle
absorption; lower trace, net metal atom absorption

Release Mounting and Vacuum

System (9-15): 9, vacuum tank; 10, shroud; 11, shroud flange and baffle;
12, release package; 13, release plume; 14, shroud flange
purge gas inlet; 15, tank purge gas inlet

Parameters used to Estimate

Yields (s, l, w):

s, distance from release to optic axis;
l, light path through release plume;
w, diam of light beam

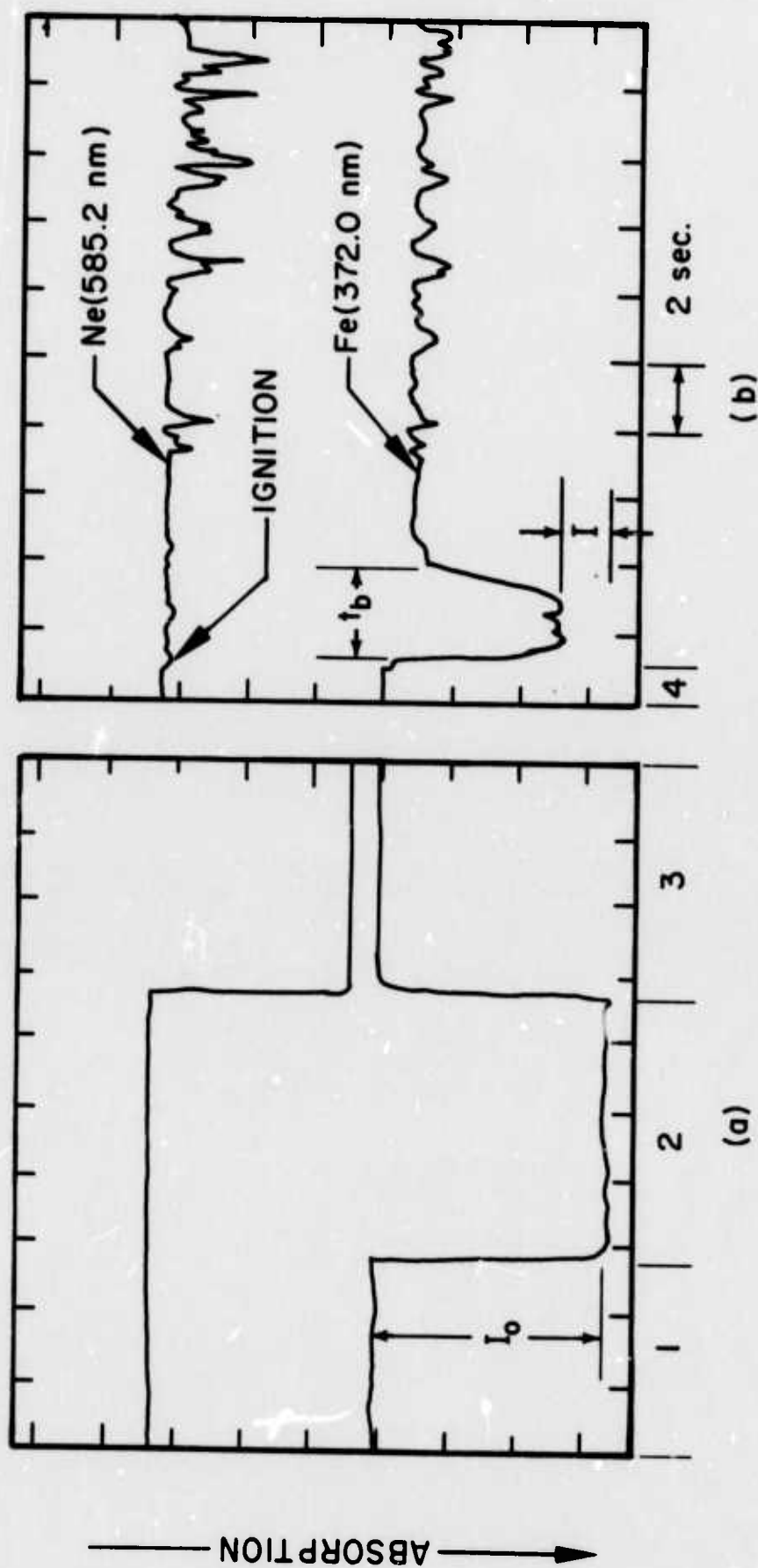


FIG. 2 CALIBRATION (a) AND MEASUREMENT (b) OSCILLOSCOPE TRACES FROM A TYPICAL RELEASE BURN

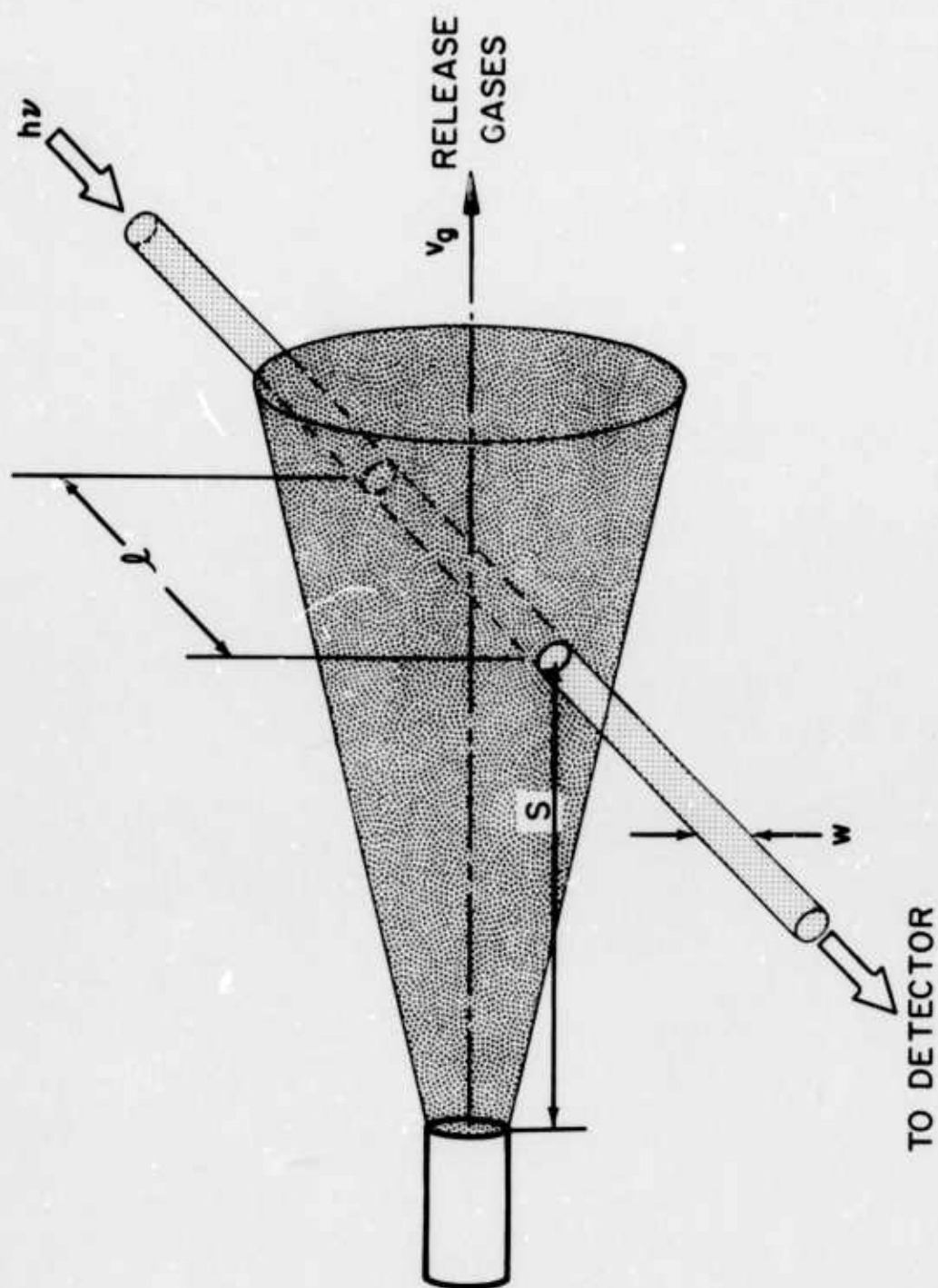


FIG. 3 GEOMETRY OF BURNING RELEASE

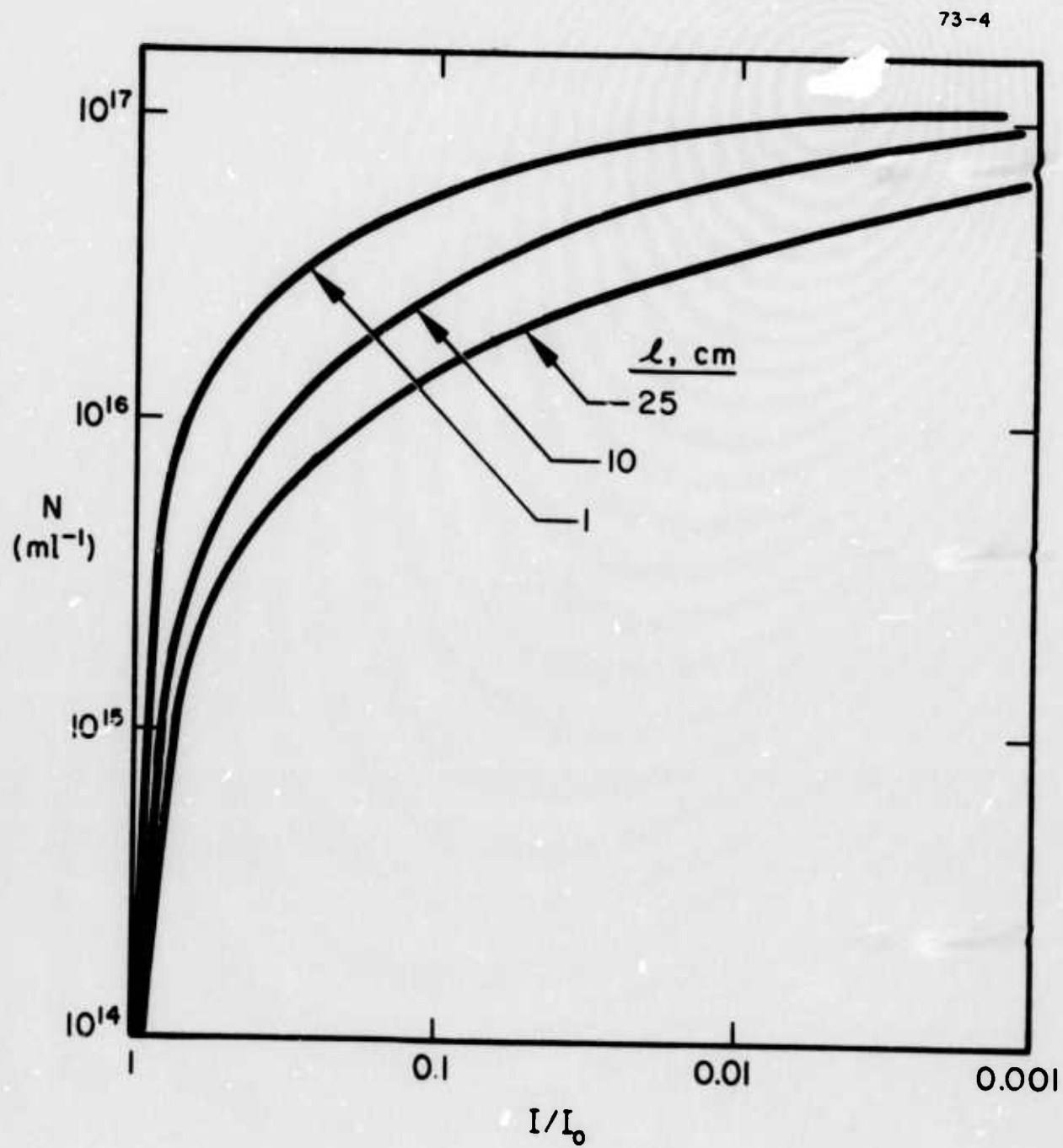


FIG. 4 INFLUENCE OF PATH LENGTH ON NUMBER DENSITY

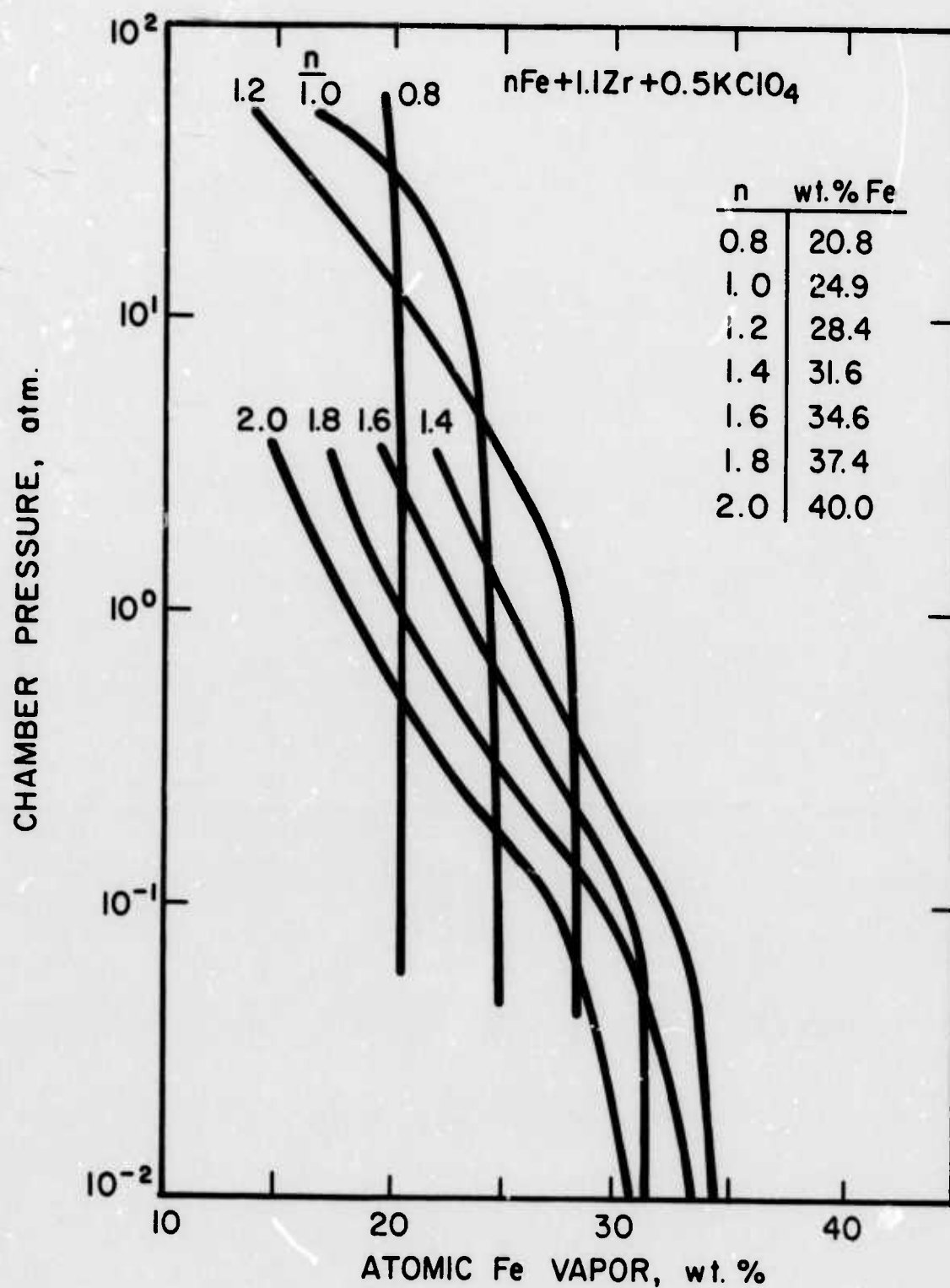


FIG. 5 INFLUENCE OF MIXTURE RATIO
ON PREDICTED ATOMIC Fe VAPOR YIELDS

KClO_4 oxidizer

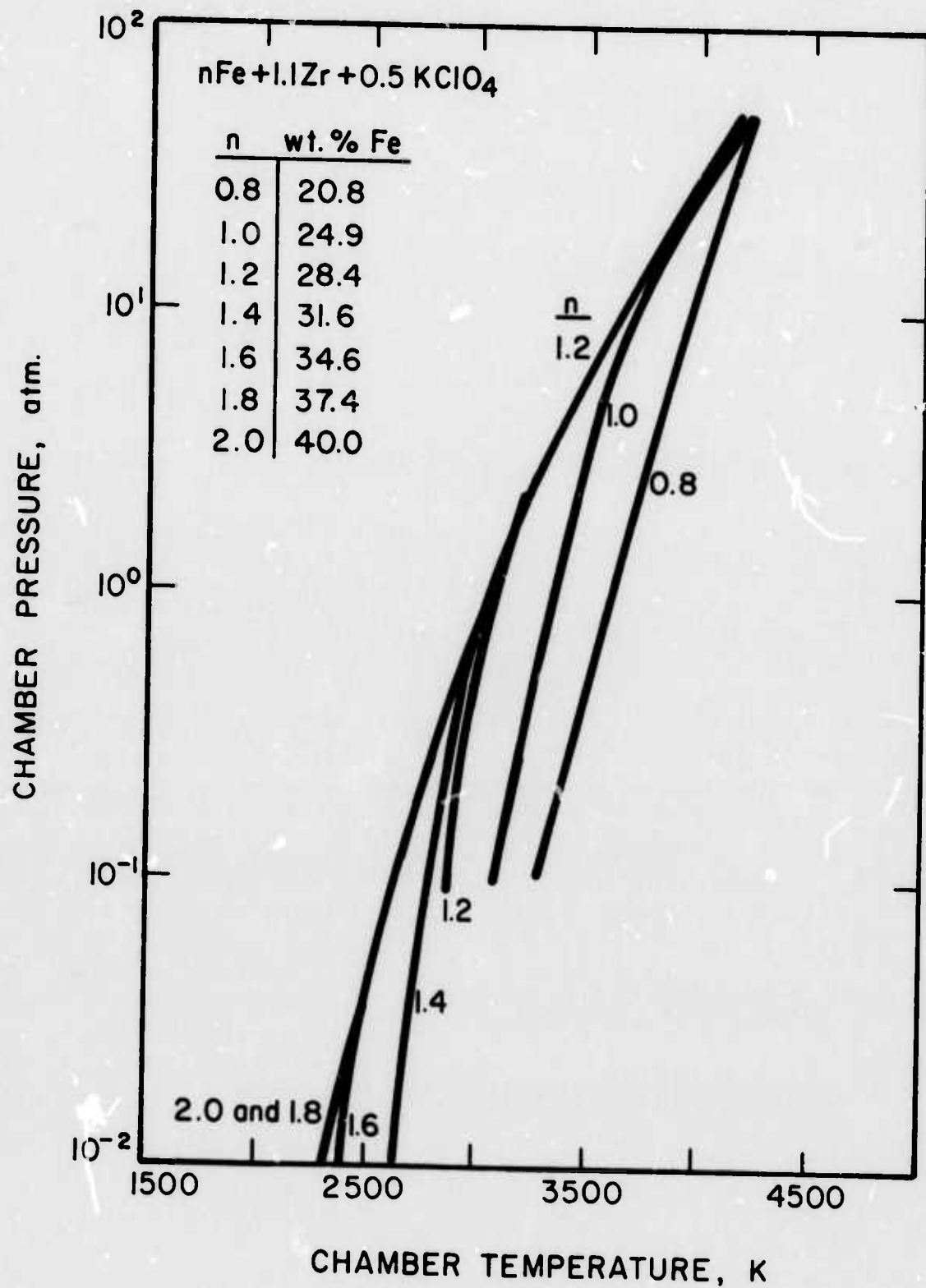


FIG. 6 INFLUENCE OF MIXTURE RATIO
ON PREDICTED CHAMBER TEMPERATURE

KClO_4 oxidizer

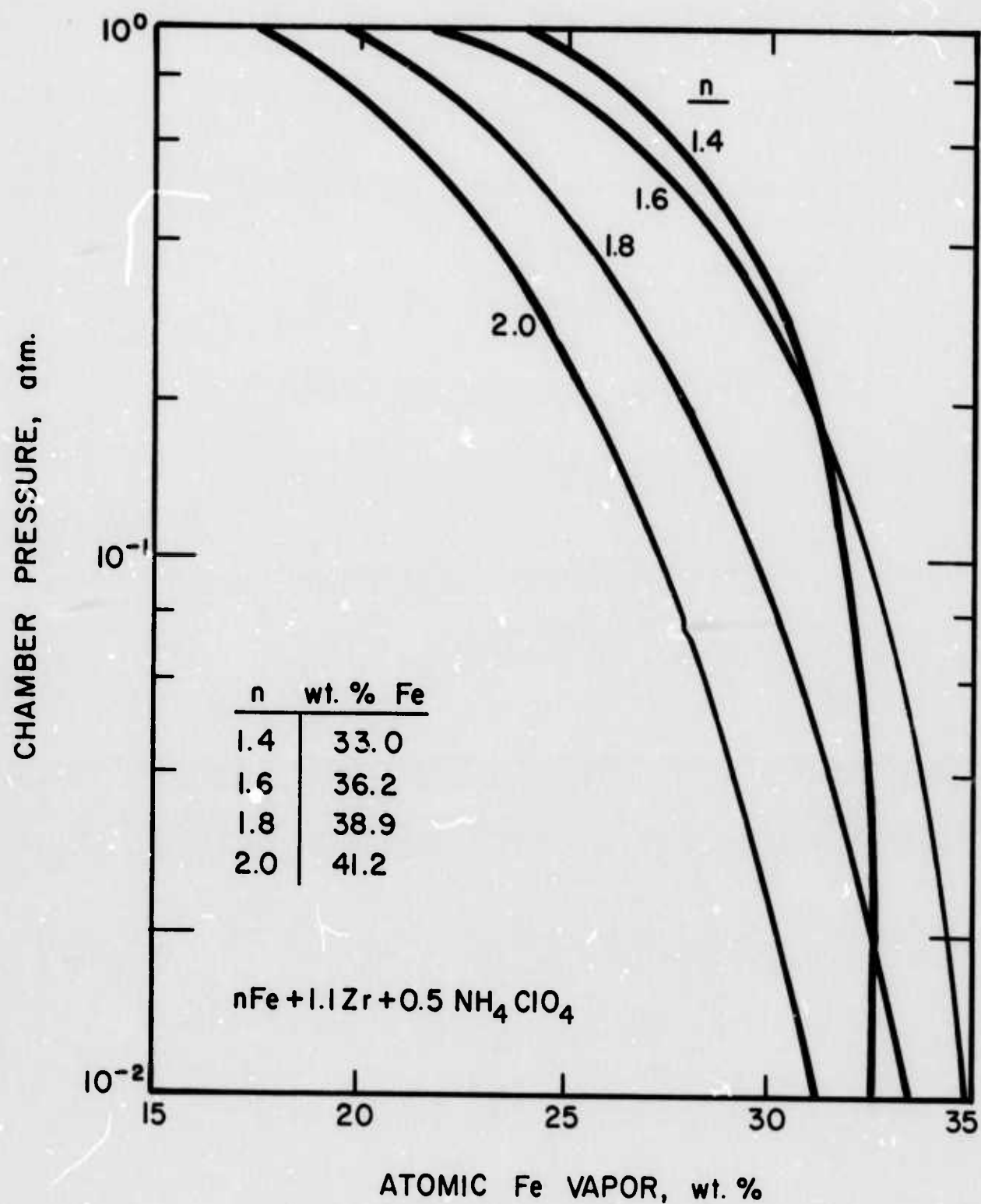


FIG. 7 INFLUENCE OF MIXTURE RATIO
ON PREDICTED ATOMIC Fe VAPOR YIELDS

NH_4ClO_4 oxidizer

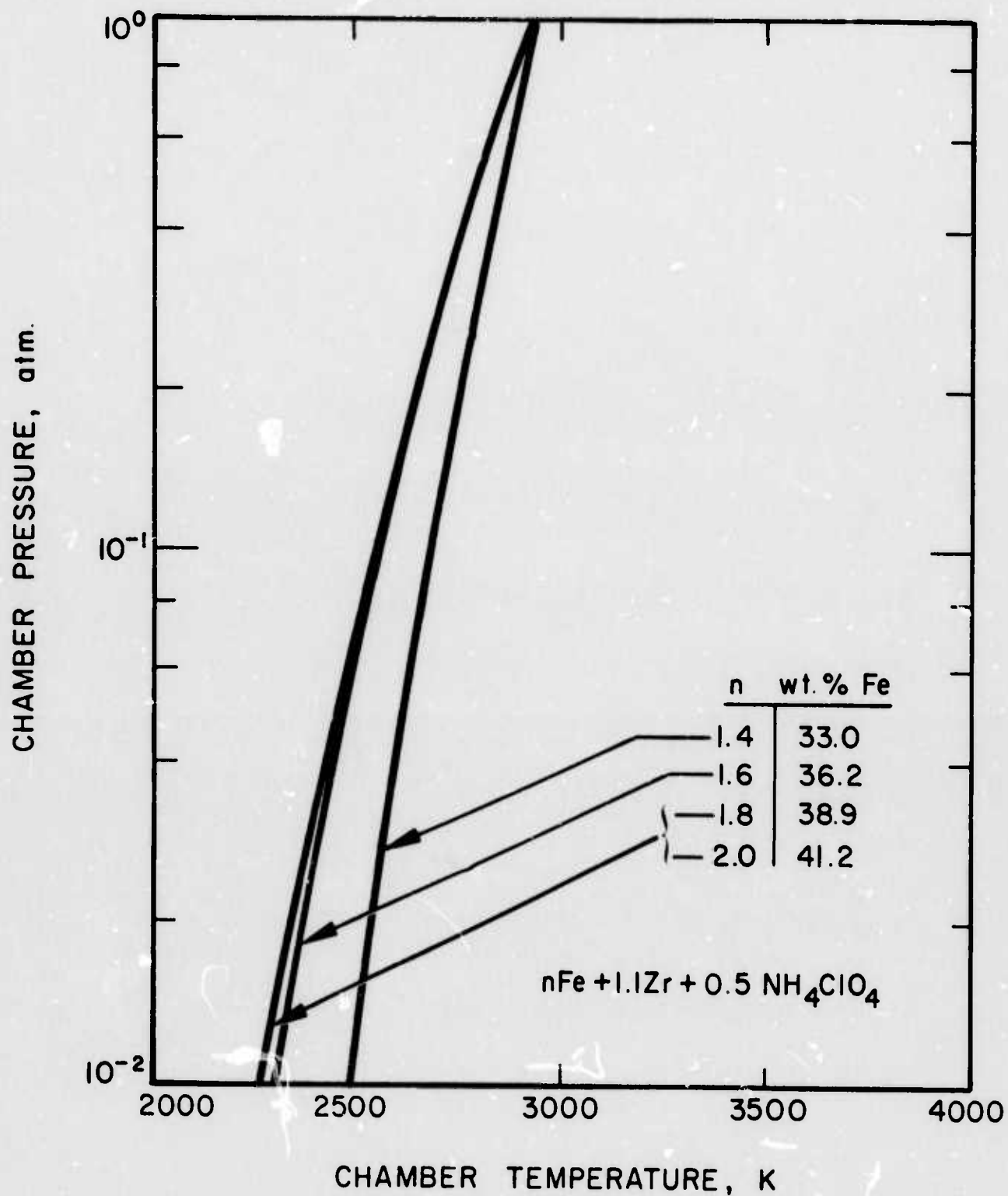


FIG. 8 INFLUENCE OF MIXTURE RATIO
ON PREDICTED CHAMBER TEMPERATURE

NH_4ClO_4 oxidizer

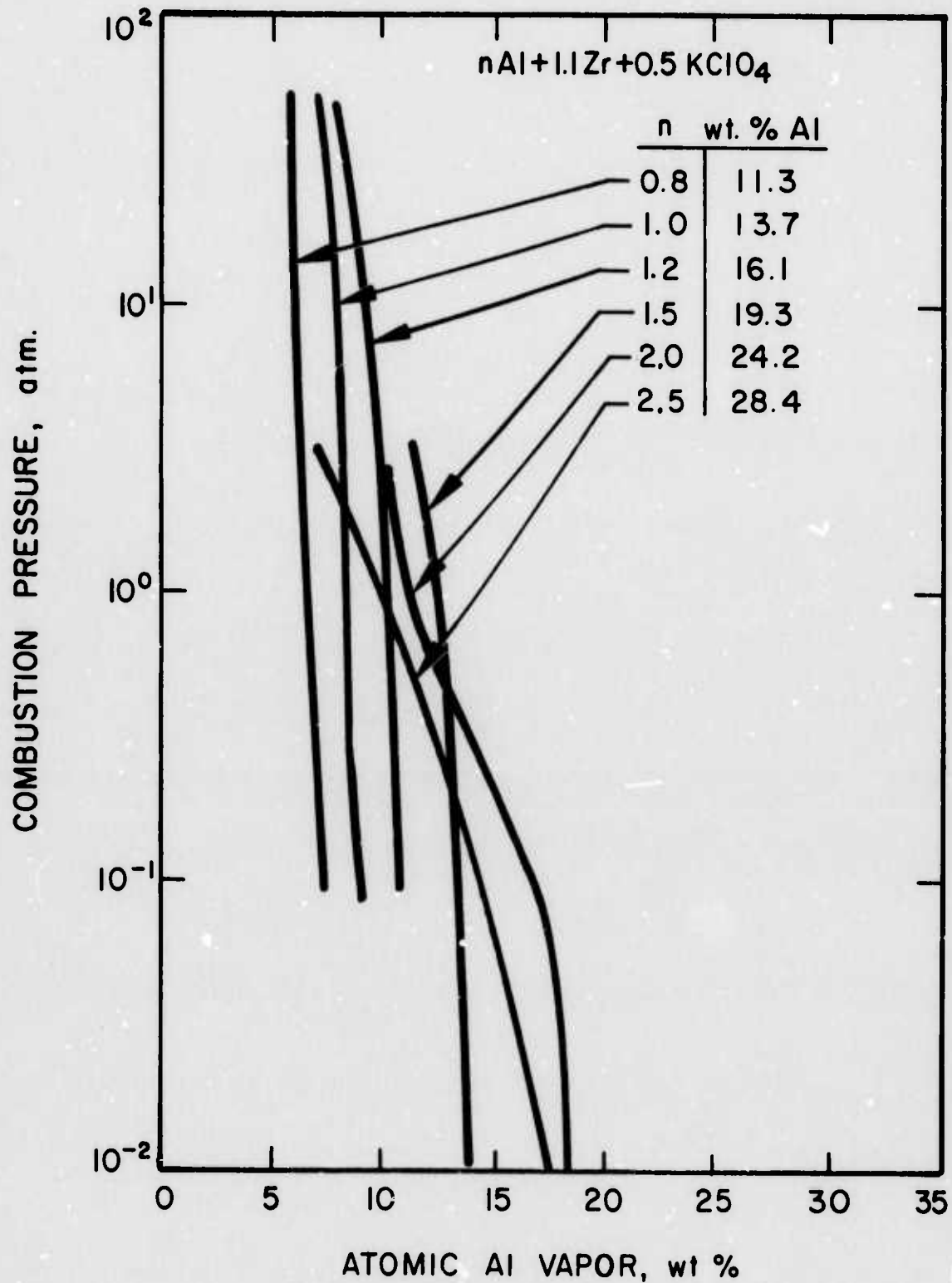


FIG. 9 INFLUENCE OF MIXTURE RATIO
ON PREDICTED ATOMIC Al VAPOR YIELDS

KClO_4 oxidizer

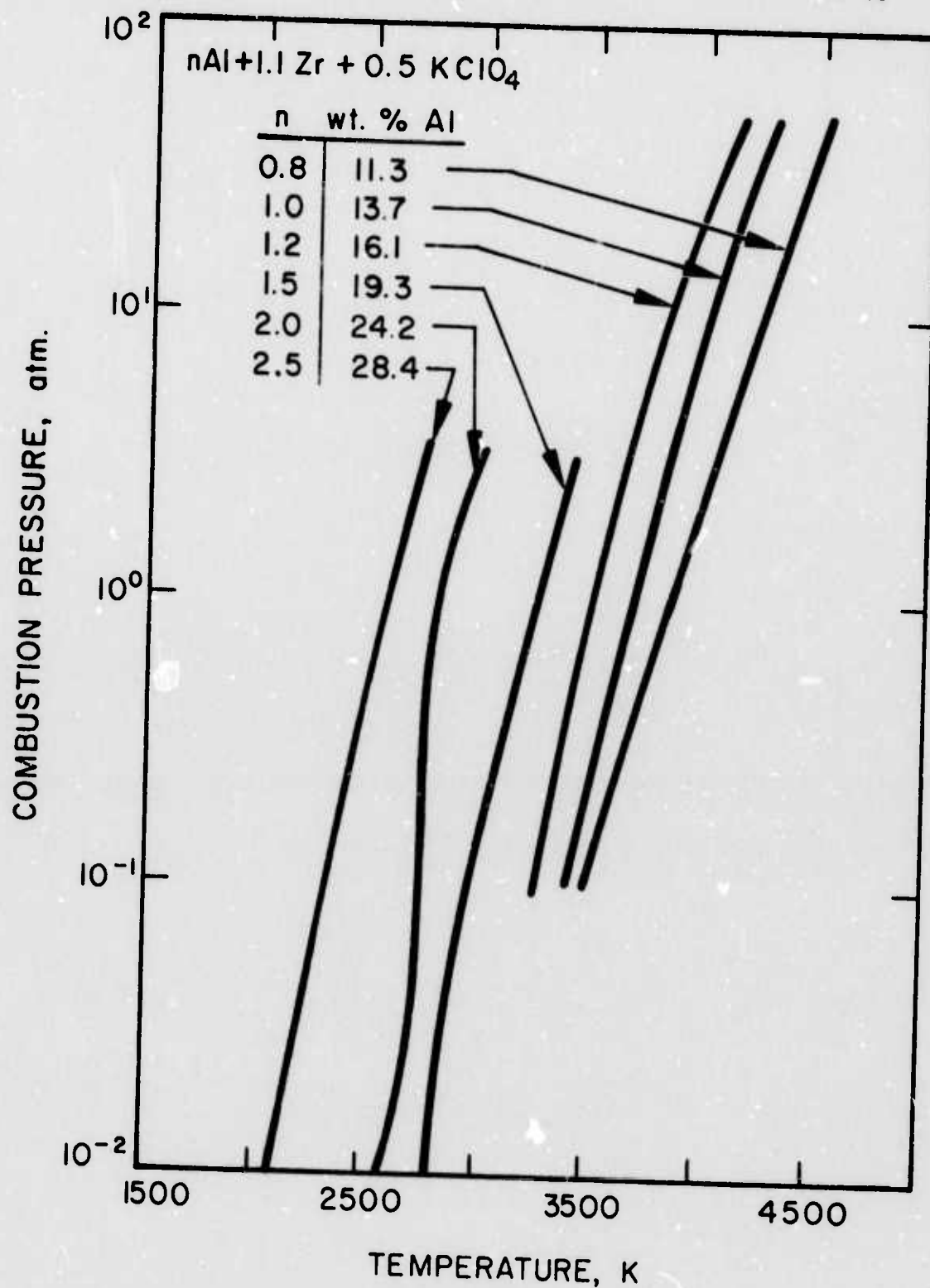


FIG. 10 INFLUENCE OF MIXTURE RATIO
ON PREDICTED CHAMBER TEMPERATURE

KClO_4 oxidizer

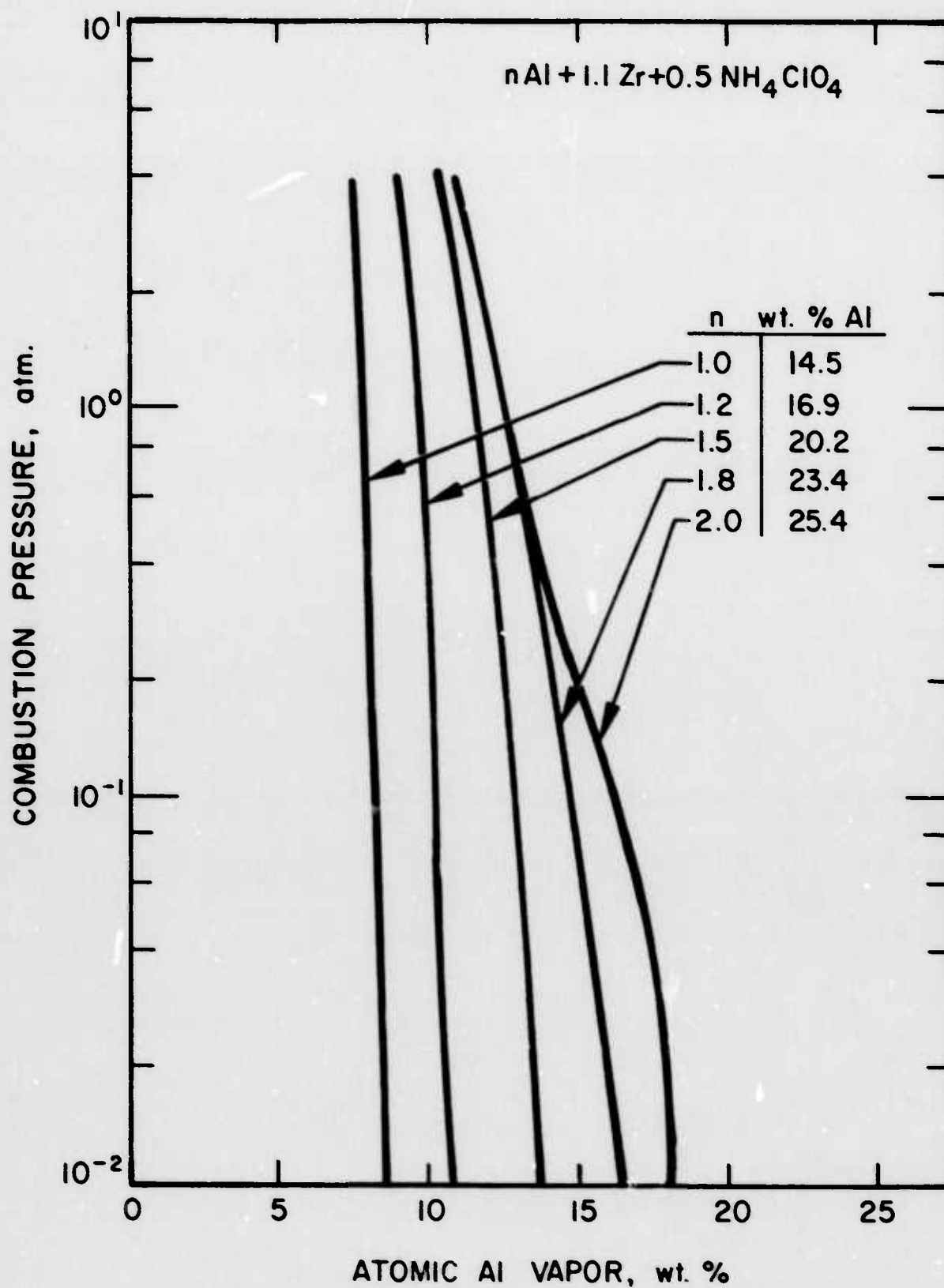


FIG. 11 INFLUENCE OF MIXTURE RATIO
ON PREDICTED ATOMIC Al VAPOR YIELDS

NH_4ClO_4 oxidizer

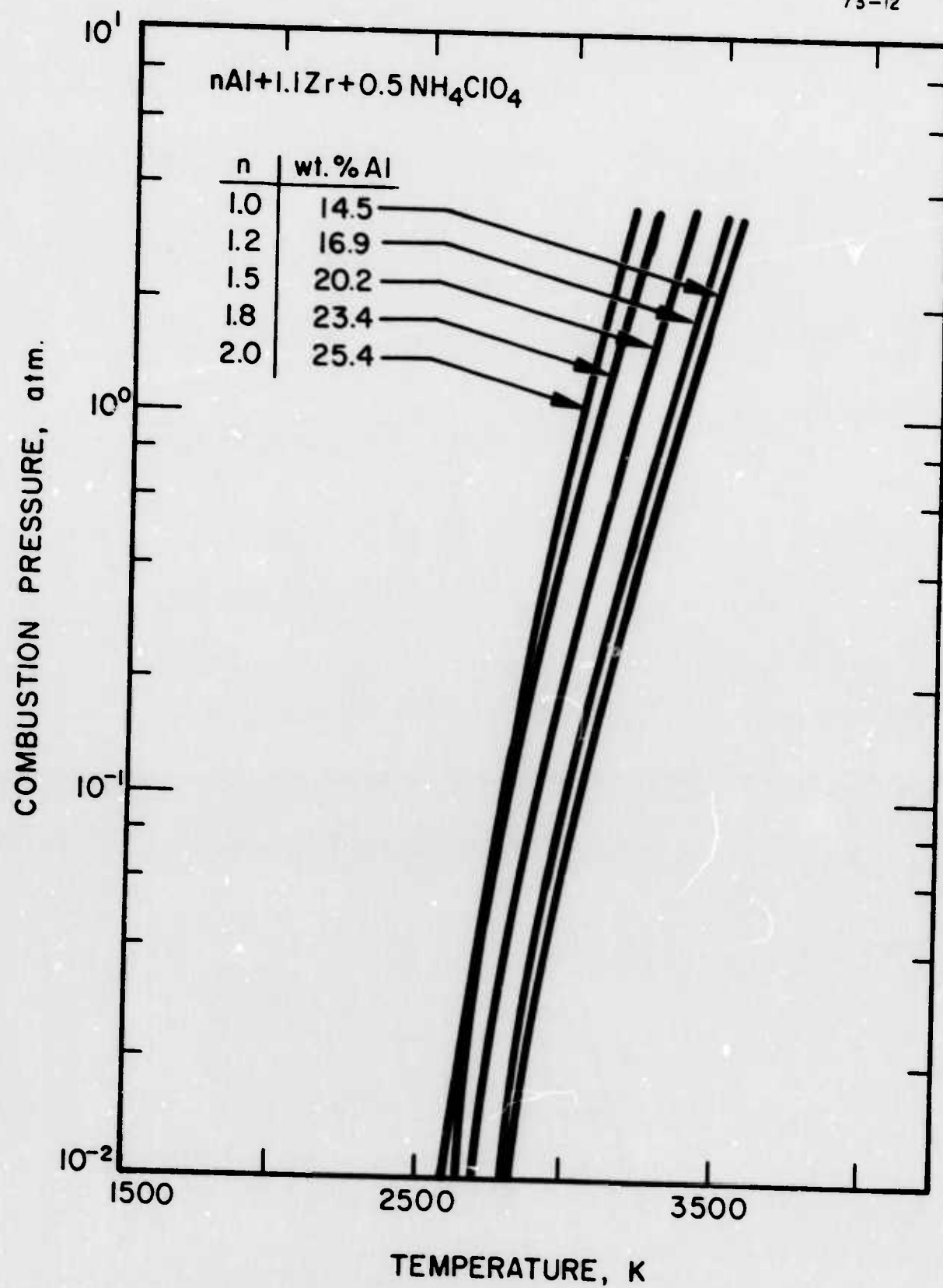


FIG. 12 INFLUENCE OF MIXTURE RATIO
ON PREDICTED CHAMBER TEMPERATURE

NH_4ClO_4 oxidizer

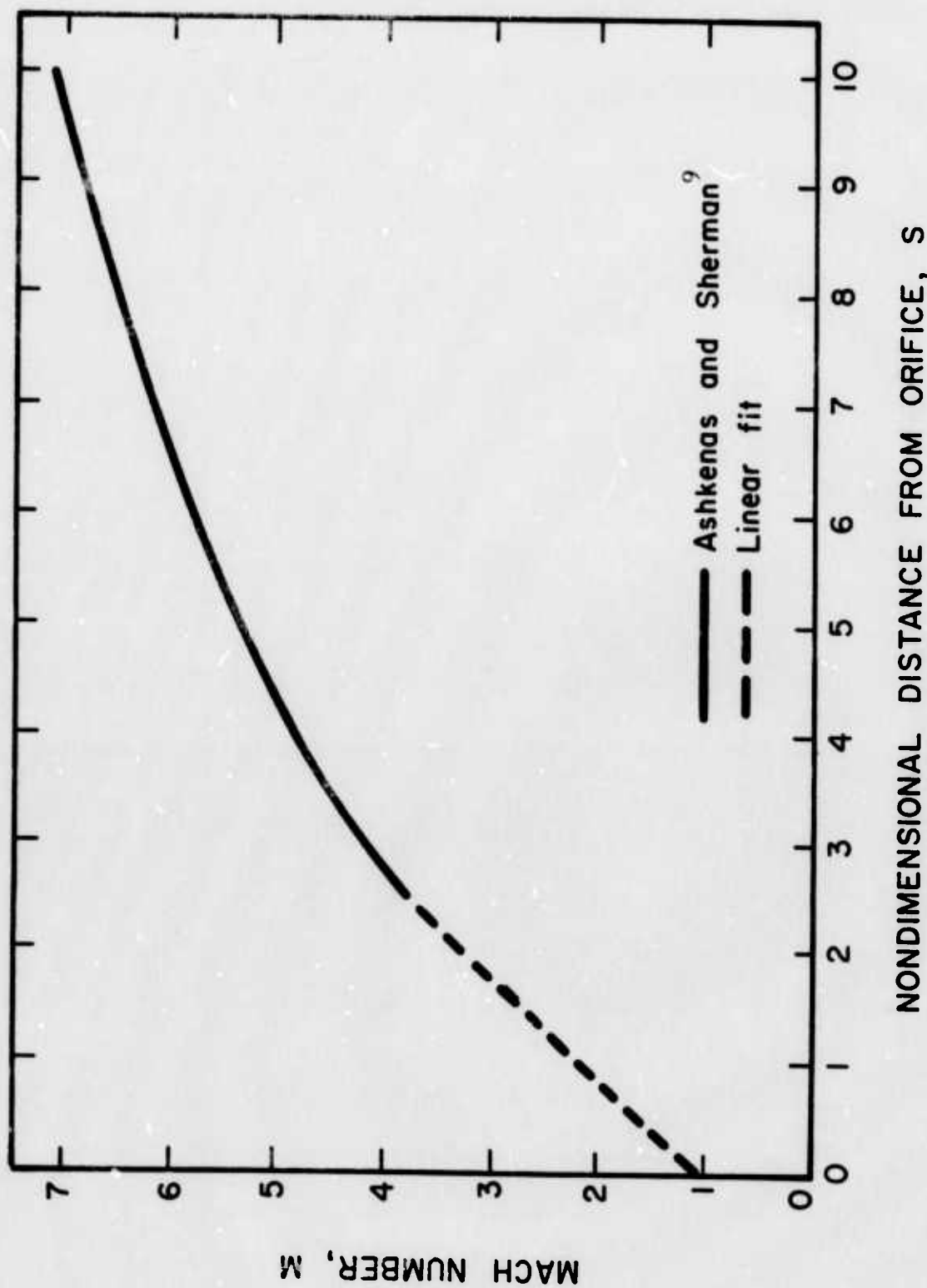


FIG. 13 CENTERLINE MACH NUMBER FOR EXPANSION OF SONIC JET INTO VACUUM

 $S = \text{distance from orifice/orifice diameter, } \gamma = 1.3$

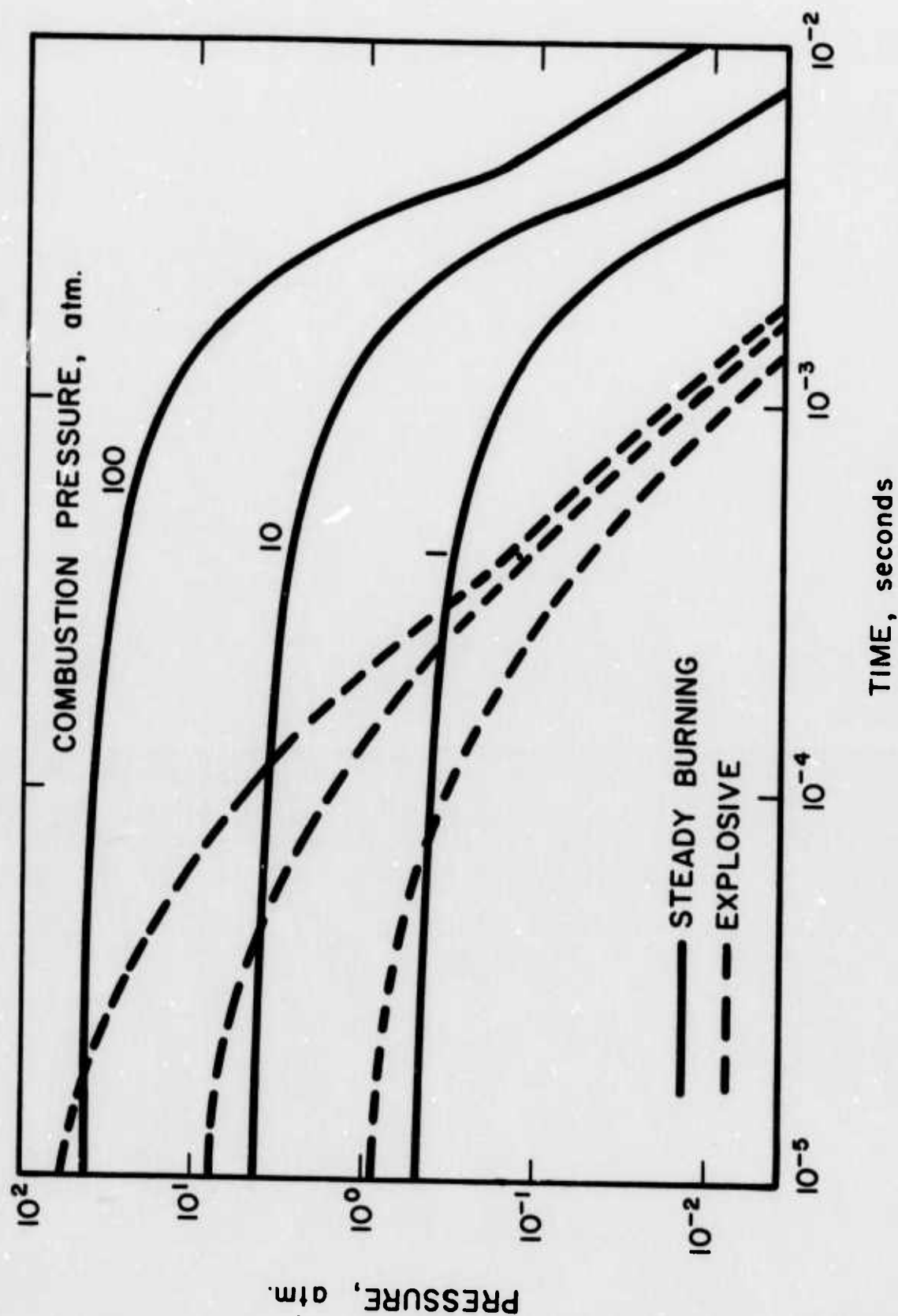


FIG. 14 COMPARISONS BETWEEN PRESSURE-TIME HISTORIES FOR STEADY-BURNING AND EXPLOSIVE RELEASES

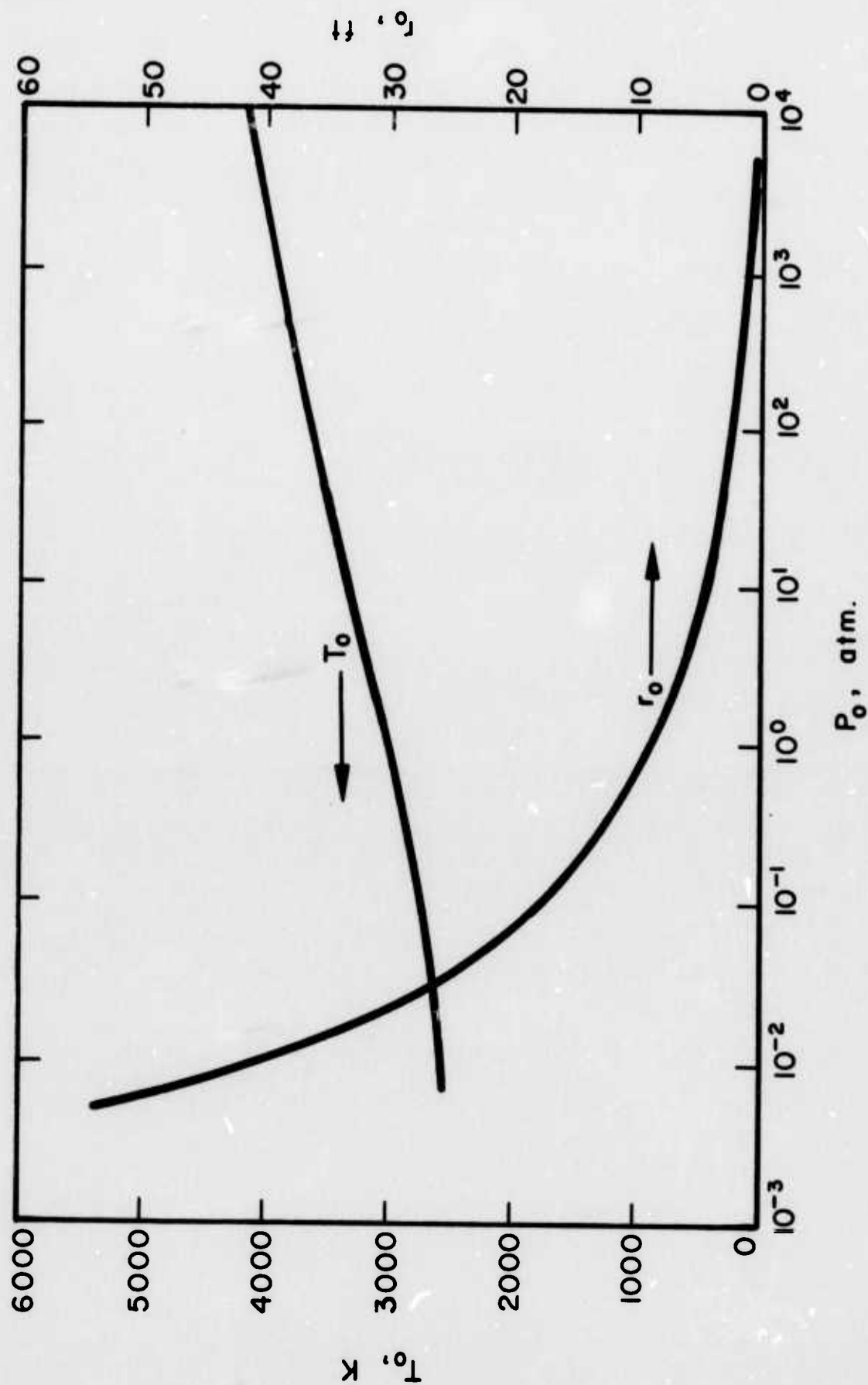


FIG. 15 RADIUS OF A SPHERE REQUIRED FOR A 20 kg
FLASHBULB EXPLOSIVE RELEASE

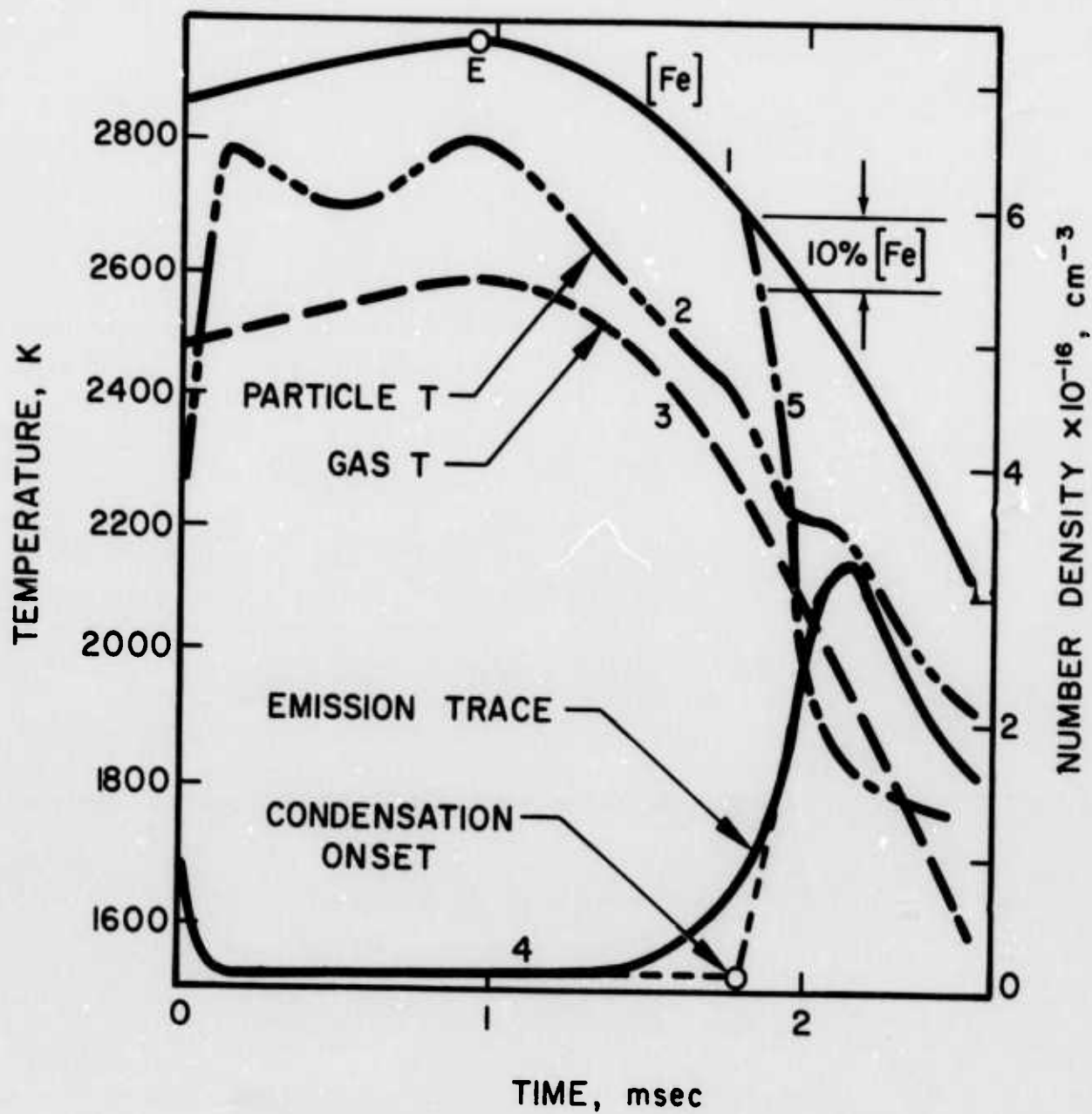


FIG. 16 GAS AND PARTICLE TEMPERATURES
AND Fe NUMBER DENSITIES IN SHOCK TUBE
MEASUREMENTS

after Kung and Bauer¹⁰

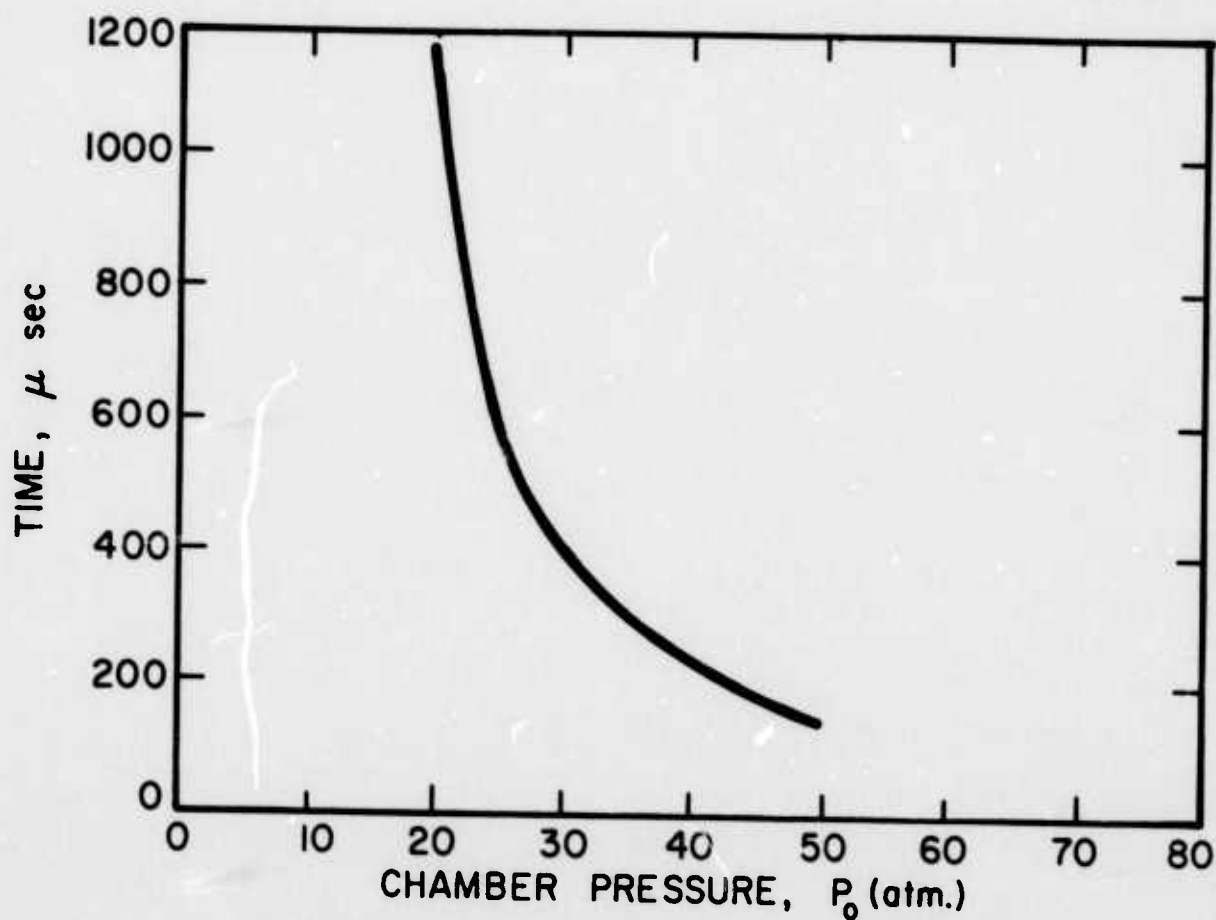


FIG. 17 FLOW TIME FOR CONDENSATION ONSET

$$f \approx 0.9, k \propto T^{-2}$$

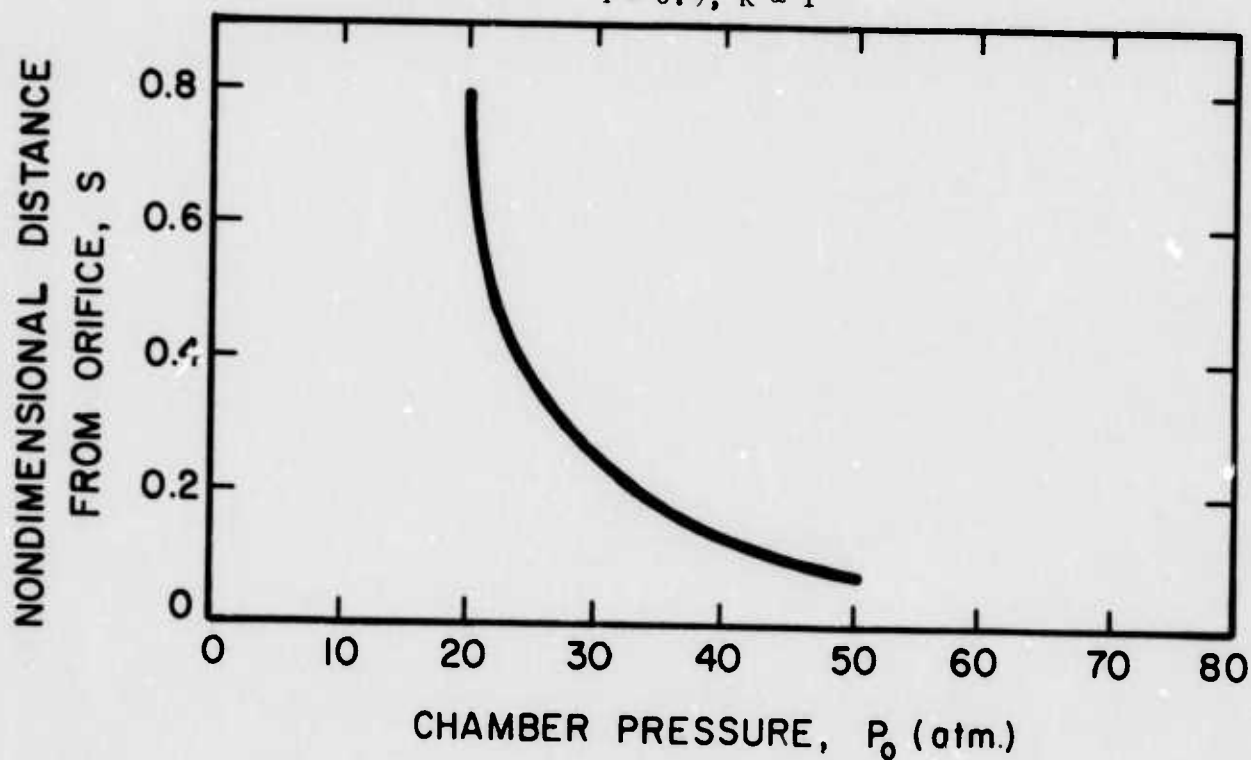


FIG. 18 POSITION OF CONDENSATION ONSET IN JET

$$f \approx 0.9, k \propto T^{-2}$$